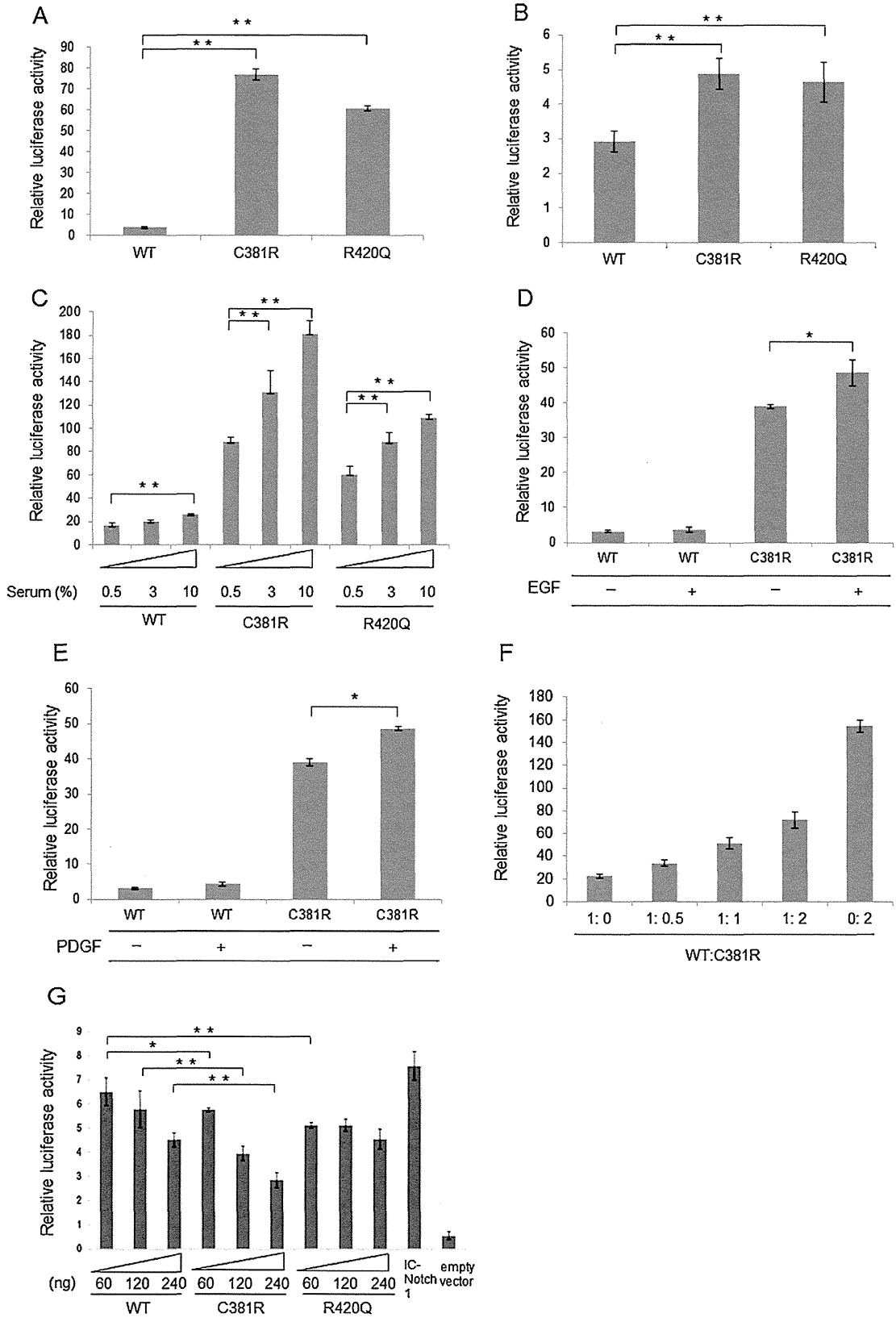

Fig. 2. ELK, c-Jun, and HES1 transactivation in cells expressing mutant CBL proteins. The results are expressed as the mean and standard deviation of mean values from triplicate samples. $^{**}P < 0.01$ and $^{*}P < 0.05$ determined with Student's *t*-test. (A) ELK transactivation in cells with WT CBL and mutant CBL. (B) c-Jun transactivation in cells with WT CBL and mutant CBL. (C) ELK transactivation in NIH 3T3 cells transiently expressing WT CBL and C381R CBL in DMEM that contained the indicated concentrations of newborn calf serum (NCS). (D) For EGF stimulation, the ELK transactivation level in cells expressing p.C381R stimulated with EGF was significantly enhanced compared

p.C381R and p.R420Q in DMEM containing 10% NCS compared with WT *CBL*-transfected cells (Fig. 2A). The transactivation of the transcription factor c-Jun was examined in NIH 3T3 cells. Studies have shown that c-Jun activity is upregulated by the phosphorylation of c-Jun NH2-terminal kinases (JNK) [25]. In this case, c-Jun transactivation was significantly enhanced in cells expressing p.C381R and p.R420Q in DMEM containing 10% NCS (Fig. 2B). These results demonstrate that *CBL* mutants activate the ERK and JNK pathways, possibly via the upstream activation of RAS in the presence of serum.

ELK transactivation was examined in different NCS concentrations to evaluate the effect of serum concentration. ELK transactivation in cells expressing p.C381R and p.R420Q was enhanced in an NCS concentration-dependent manner (Fig. 2C). Significant ELK activation was observed in cells expressing p.C381R and p.R420Q in DMEM with 0.5% NCS. The effects of EGF and PDGF on ELK transactivation were examined in cells expressing WT *CBL* or p.C381R *CBL*. The ELK transactivation levels in cells expressing p.C381R that were stimulated with 100 ng/ml EGF (Fig. 2D) or 100 ng/ml PDGF (Fig. 2E) were significantly enhanced compared with those of unstimulated cells. However, EGF and PDGF stimulation did not significantly alter the ELK transactivation levels in cells expressing WT *CBL*. These results suggest that the p.C381R mutation constitutively activates the RAS pathway.

CBL mutations affect endogenous WT CBL in a dominant-negative manner [7]. NIH 3T3 cells were co-transfected with WT CBL and C381R to evaluate the effect of p.C381R on WT CBL. The hypertransactivation response that was induced by the CBL mutant was abolished by the co-transfection of WT CBL (Fig. 2F), suggesting the pathogenic importance of the WT *CBL* allele loss.

3.5. *HES transactivation in cells expressing mutant CBL*

HES1 is a target gene for NOTCH1. WT or mutant CBL constructs were transiently transfected in NIH 3T3 cells with the HES-Luc reporter and a constitutively active intracellular domain of NOTCH1 (ICN1) construct. ICN1 expression significantly increased the transactivation of HES (Fig. 2G, IC-NOTCH1 lane). The introduction of CBL WT or mutants significantly reduced the HES transactivation levels compared with cells expressing ICN1 (Fig. 2G). The HES1 transactivation levels in cells expressing p.C381R were significantly decreased compared with CBL WT-expressing cells.

4. Discussion

In this study, a homozygous p.C381R mutation and a UPD of the region that included *CBL* were identified in T-ALL cells, and a heterozygous germline p.W408R mutation was identified in one patient with JMML. An additional mutation analysis identified two *NOTCH1* mutations and homozygous deletions of *LEF1* and *CDKN2A* in T-ALL cells. A functional analysis revealed that cells expressing the p.C381R mutant constitutively transactivated ELK and c-Jun. Co-transfection of WT and the p.C381R mutation in NIH 3T3 cells revealed that WT inhibited the ELK-activating effects of p.C381R. The HES1 transactivation levels in cells expressing p.C381R were significantly decreased compared with CBL WT-expressing cells, suggesting that this *CBL* mutation plays a role in NOTCH signaling pathway.

CBL mutations are rare in ALL patients. Recently, mutations in *CBL* have been identified in 2 infant ALL patients with *MLL* gene rearrangements [26]. Nicholson et al. analyzed the linker-RING domains of CBL in a cohort of 180 diagnostic and 46 relapsed ALL patients and identified deletions/insertions of *CBL*, including the splicing acceptor or donor site of exon 8 in three ALL samples [27]. *CBL* mutations in ALL may promote the proliferation of leukemia cells by activating the RAS pathway ([27] and our study). Alternatively, our HES-reporter assay in cells that expressed the *NOTCH1* constitutive active mutant showed that *CBL* p.C381R downregulated the NOTCH1 signaling pathway, suggesting that the *CBL* p.C381R mutation may contribute to leukemogenesis through interaction with NOTCH1. The relationship between CBL and NOTCH1 has not been elucidated, but one report has demonstrated that CBL promotes the ubiquitin-dependent lysosomal degradation of membrane-associated NOTCH1 [28]. In the case of NOTCH3, its interactions with pre-TCR lead to the recruitment and persistence of the CBL to the lipid rafts in thymocytes from mice expressing the constitutively active intracellular domain of NOTCH3, which suggests that CBL may regulate the NOTCH3 and pre-TCR relationship during T-cell leukemogenesis [29]. Further analysis will elucidate the role of the *CBL* mutation in T-ALL leukemogenesis.

Somatic and germline *CBL* mutations have been clustered in either the linker domain or the RING finger domain (Fig. 3). The loss of the ubiquitination of activated receptor tyrosine kinases is thought to contribute to the transforming potential of leukemia-associated mutant CBL proteins. The distributions of somatic and germline mutations were almost similar. However, Y371, which is a hot spot for *CBL* mutations in JMML, is rarely mutated in other myeloid malignancies [5]. The germline p.W408R mutation has been identified in a patient with JMML [5]. Individuals with germline *CBL* mutations display a variable combination of dysmorphic features, including mild hypertelorism, a short upturned nose, a deeply grooved philtrums and thick lips, which are reminiscent of the facial gestalt of NS [10]. Patient PL52, who had a germline p.W408R mutation, had normal development and no dysmorphic features at 15 months of age. However, her young age may have precluded any firm conclusions. Long-term follow-up examinations and an analysis of wider cohorts is necessary to further characterize the phenotypic spectrum that is associated with germline mutations in *CBL*.

The effect of mutant CBLs on ERK activation depends on the level of endogenous WT CBL [7,30]. Therefore, we examined ELK transactivation in NIH 3T3 cells, which have low endogenous CBL protein expression [31]. Our study demonstrated that ELK transactivation in cells expressing p.C381R decreased with increasing WT CBL expression. These results suggest that the p.C381R mutation functions in a dominant-negative manner or as a gain-of-function mutation.

In this study, SNP array analyses of samples from leukemia cells and leukocytes obtained from patients in remission revealed a copy number imbalance that was specific for leukemia cells. The homozygous deletion of the entire *LEF1* gene was identified in the T-ALL sample with the *CBL* mutation. LEF1 is a member of the lymphoid enhancer factor/T-cell factor family of DNA-binding transcription factors that interact with nuclear β-catenin in the WNT signaling pathway [32]. Monoallelic or biallelic *LEF1* microdeletions have been identified in 11% (5 of 47) of primary samples from the diagnostic specimens of 47 children with T-ALL, using high-resolution array comparative genomic hybridization [33]. The homozygous deletion of *CDKN2A* and

with unstimulated cells. (E) For PDGF stimulation, the ELK transactivation level in cells expressing p.C381R stimulated with 100 ng/ml PDGF was enhanced compared with unstimulated cells. (F) Co-transfection of WT CBL and C381R CBL. The hypertransactivation response induced by CBL p.C381R was abolished by the co-transfection of WT CBL. (G) Mutant CBL constructs in pCMV6 were transiently transfected in NIH 3T3 cells with the HES-Luc reporter and the intracellular NOTCH1 (ICN1) construct where appropriate.

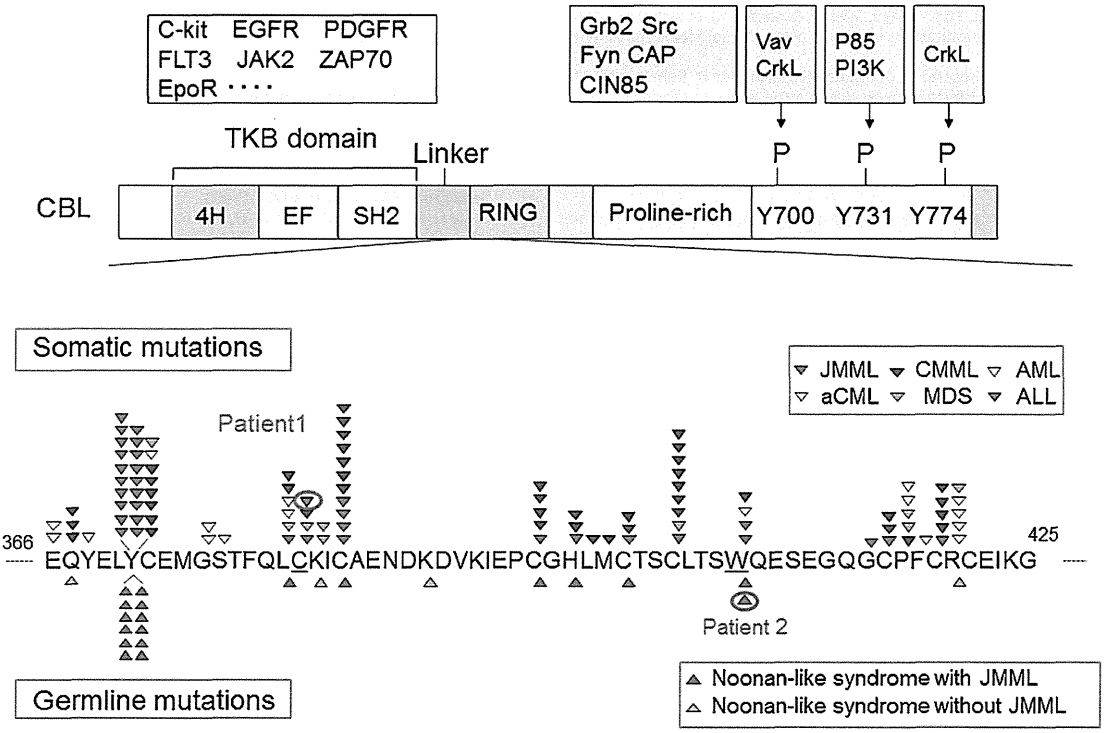

Fig. 3. The CBL structure and mutation spectrum. CBL comprises an N-terminal tyrosine kinase binding domain (TKB) connected by a linker to the RING-finger domain implicated in E2 enzyme binding. These domains are followed by a proline-rich region and a C-terminal portion containing tyrosine phosphorylation sites. The molecular interaction of CBL with cytokine receptors and other signaling molecules are also shown on top. The *CBL* mutations identified in hematologic malignancies partially overlap with those identified in the germline.

CDKN2B, which are frequently inactivated in various hematological malignancies [34], was also identified in the T-ALL sample. A comparison of the copy numbers of DNA samples from leukemia cells and germline DNA will help to highlight the abnormalities in leukemia.

In conclusion, we identified a *CBL* p.C381R mutation in leukemia cells from one patient with T-ALL. A functional analysis demonstrated that the mutation constitutively activated the RAS-MAPK pathway and inhibited the constitutive activation of the NOTCH signaling pathway. Further studies will be needed to determine the relationship between CBL and leukemogenesis.

Conflict of interest statement

All authors declare no competing financial interests.

Acknowledgments

The authors thank the patients, their families and the doctors who participated in this study. We are grateful to Dr. Tasuku Honjo at Kyoto University for supplying the HES-Luc expression construct in pGV-B and mouse intracellular NOTCH1 region expression construct in pEF-BOSneo. We are also grateful to Drs. Kunihiko Moriya and Naoto Ishii for their helpful discussions. We thank Kumi Kato, Yoko Tateda and Riyo Takahashi for their technical assistance. This work was supported by the Funding Program for the Next Generation of World-Leading Researchers (NEXT Program) from the Ministry of Education, Culture, Sports, Science and Technology of Japan to YA and from the Ministry of Health, Labor and Welfare to YM and YA. This work was supported in part by the National Cancer Center Research and Development FUND (23-22-11).

Contributions. YS, YA and SK designed the research study; YS, HM, HM and TN performed the research; MI, TR, YS, ST and SK provided patients samples; YS, HM, HM and JPM analyzed the data; YS, YA and YM wrote the paper.

Appendix A. Supplementary data

Supplementary data associated with this article can be found, in the online version, at http://dx.doi.org/10.1016/j.leukres.2012.04.018.

References

[1] Langdon WY, Hartley JW, Klinken SP, Ruscetti SK, Morse 3rd HC. v-cbl, an oncogene from a dual-recombinant murine retrovirus that induces early B-lineage lymphomas. Proc Natl Acad Sci USA 1989;86:1168–72.
[2] Schmidt MH, Dikic I. The Cbl interactome and its functions. Nat Rev Mol Cell Biol 2005;6:907–18.
[3] Dunbar AJ, Gondek LP, O'Keefe CL, Makishima H, Rataul MS, Szpurka H, et al. 250K single nucleotide polymorphism array karyotyping identifies acquired uniparental disomy and homozygous mutations, including novel missense substitutions of c-Cbl, in myeloid malignancies. Cancer Res 2008;68:10349–57.
[4] Grand FH, Hidalgo-Curtis CE, Ernst T, Zoi K, Zoi C, McGuire C, et al. Frequent CBL mutations associated with 11q acquired uniparental disomy in myeloproliferative neoplasms. Blood 2009;113:6182–92.
[5] Loh ML, Sakai DS, Flotho C, Kang M, Fliegauf M, Archambeault S, et al. Mutations in CBL occur frequently in juvenile myelomonocytic leukemia. Blood 2009;114:1859–63.
[6] Muramatsu H, Makishima H, Jankowska AM, Cazzolli H, O'Keefe C, Yoshida N, et al. Mutations of an E3 ubiquitin ligase c-Cbl but not TET2 mutations are pathogenic in juvenile myelomonocytic leukemia. Blood 2010;115:1969–75.
[7] Sanada M, Suzuki T, Shih LY, Otsu M, Kato M, Yamazaki S, et al. Gain-of-function of mutated C-CBL tumour suppressor in myeloid neoplasms. Nature 2009;460:904–8.

[8] Caligiuri MA, Briesewitz R, Yu J, Wang L, Wei M, Arnoczky KJ, et al. Novel c-CBL and CBL-b ubiquitin ligase mutations in human acute myeloid leukemia. Blood 2007;110:1022–4.
[9] Sargin B, Choudhary C, Crosetto N, Schmidt MH, Grundler R, Rensinghoff M, et al. Flt3-dependent transformation by inactivating c-Cbl mutations in AML. Blood 2007;110:1004–12.
[10] Perez B, Mechinaud F, Galambrun C, Ben Romdhane N, Isidor B, Philip N, et al. Germline mutations of the CBL gene define a new genetic syndrome with predisposition to juvenile myelomonocytic leukaemia. J Med Genet 2010;47:686–91.
[11] Niemeyer CM, Kang MW, Shin DH, Furlan I, Erlacher M, Bunin NJ, et al. Germline CBL mutations cause developmental abnormalities and predispose to juvenile myelomonocytic leukemia. Nat Genet 2010;42:794–800.
[12] Martinelli S, De Luca A, Stellacci E, Rossi C, Checquolo S, Lepri F, et al. Heterozygous germline mutations in the CBL tumor-suppressor gene cause a Noonan syndrome-like phenotype. Am J Hum Genet 2010;87:250–7.
[13] Aoki Y, Niihori T, Narumi Y, Kure S, Matsubara Y. The RAS/MAPK syndromes: novel roles of the RAS pathway in human genetic disorders. Hum Mutat 2008;29:992–1006.
[14] Tidyman WE, Rauen KA. The RASopathies: developmental syndromes of Ras/MAPK pathway dysregulation. Curr Opin Genet Dev 2009;19:230–6.
[15] Gondek LP, Tiu R, Haddad AS, O'Keefe CL, Sekeres MA, Theil KS, et al. Single nucleotide polymorphism arrays complement metaphase cytogenetics in detection of new chromosomal lesions in MDS. Leukemia 2007;21:2058–61.
[16] Kurooka H, Kuroda K, Honjo T. Roles of the ankyrin repeats and C-terminal region of the mouse notch1 intracellular region. Nucleic Acids Res 1998;26:5448–55.
[17] Kato H, Sakai T, Tamura K, Minoguchi S, Shirayoshi Y, Hamada Y, et al. Functional conservation of mouse Notch receptor family members. FEBS Lett 1996;395:221–4.
[18] Komatsuzaki S, Aoki Y, Niihori T, Okamoto N, Hennekam RC, Hopman S, et al. Mutation analysis of the SHOC2 gene in Noonan-like syndrome and in hematologic malignancies. J Hum Genet 2010;55:801–9.
[19] Weng AP, Ferrando AA, Lee W, Morris JP, Silverman LB, Sanchez-Irizarry C, et al. Activating mutations of NOTCH1 in human T cell acute lymphoblastic leukemia. Science 2004;306:269–71.
[20] O'Neil J, Grim J, Strack P, Rao S, Tibbitts D, Winter C, et al. FBW7 mutations in leukemic cells mediate NOTCH pathway activation and resistance to gamma-secretase inhibitors. J Exp Med 2007;204:1813–24.
[21] Thompson BJ, Jankovic V, Gao J, Buonamici S, Vest A, Lee JM, et al. Control of hematopoietic stem cell quiescence by the E3 ubiquitin ligase Fbw7. J Exp Med 2008;205:1395–408.
[22] Maser RS, Choudhury B, Campbell PJ, Feng B, Wong KK, Protopopov A, et al. Chromosomally unstable mouse tumours have genomic alterations similar to diverse human cancers. Nature 2007;447:966–71.
[23] Rocquain J, Carbuccia N, Trouplin V, Raynaud S, Murati A, Nezri M, et al. Combined mutations of ASXL1, CBL, FLT3, IDH1, IDH2, JAK2, KRAS, NPM1, NRAS, RUNX1, TET2 and WT1 genes in myelodysplastic syndromes and acute myeloid leukemias. BMC Cancer 2010;10:401.
[24] Gille H, Kortenjann M, Thomae O, Moomaw C, Slaughter C, Cobb MH, et al. ERK phosphorylation potentiates Elk-1-mediated ternary complex formation and transactivation. EMBO J 1995;14:951–62.
[25] Barr RK, Bogoyevitch MA. The c-Jun N-terminal protein kinase family of mitogen-activated protein kinases (JNK MAPKs). Int J Biochem Cell Biol 2001;33:1047–63.
[26] Shiba N, Park MJ, Taki T, Takita J, Hiwatari M, Kanazawa T, et al. CBL mutations in infant acute lymphoblastic leukaemia. Br J Haematol 2012;156:672–4.
[27] Nicholson L, Knight T, Matheson E, Minto L, Case M, Sanichar M, et al. Casitas B lymphoma mutations in childhood acute lymphoblastic leukemia. Genes Chromosomes Cancer 2012;51:250–6.
[28] Jehn BM, Dittert I, Beyer S, von der Mark K, Bielke W. c-Cbl binding and ubiquitin-dependent lysosomal degradation of membrane-associated Notch1. J Biol Chem 2002;277:8033–40.
[29] Checquolo S, Palermo R, Cialfi S, Ferrara G, Oliviero C, Talora C, et al. Differential subcellular localization regulates c-Cbl E3 ligase activity upon Notch3 protein in T-cell leukemia. Oncogene 2010;29:1463–74.
[30] Ogawa S, Shih LY, Suzuki T, Otsu M, Nakauchi H, Koeffler HP, et al. Deregulated intracellular signaling by mutated c-CBL in myeloid neoplasms. Clin Cancer Res 2010;16:3825–31.
[31] Lo FY, Tan YH, Cheng HC, Salgia R, Wang YC. An E3 ubiquitin ligase: c-Cbl: a new therapeutic target of lung cancer. Cancer 2011;117:5344–50.
[32] van Noort M, Clevers H. TCF transcription factors, mediators of Wnt-signaling in development and cancer. Dev Biol 2002;244:1–8.
[33] Gutierrez A, Sanda T, Ma W, Zhang J, Grebliunaite R, Dahlberg S, et al. Inactivation of LEF1 in T-cell acute lymphoblastic leukemia. Blood 2010;115:2845–51.
[34] Ruas M, Peters G. The p16INK4a/CDKN2A tumor suppressor and its relatives. Biochim Biophys Acta 1998;1378:F115–77.

J Neuropathol Exp Neurol

Vol. 71, No. 9
September 2012
pp. 779–788

ORIGINAL ARTICLE

FUS/TLS-Immunoreactive Neuronal and Glial Cell Inclusions Increase With Disease Duration in Familial Amyotrophic Lateral Sclerosis With an R521C *FUS/TLS* Mutation

Naoki Suzuki, MD, PhD, Shinsuke Kato, MD, PhD, Masako Kato, MD, PhD, Hitoshi Warita, MD, PhD, Hideki Mizuno, MD, PhD, Masaaki Kato, MD, PhD, Naoko Shimakura, Haruhiko Akiyama, MD, PhD, Zen Kobayashi, MD, Hidehiko Konno, MD, PhD, and Masashi Aoki, MD, PhD

Abstract

Basophilic inclusions (BIs) are pathological features of a subset of frontotemporal lobar degeneration disorders, including sporadic amyotrophic lateral sclerosis (ALS) and familial ALS (FALS). Mutations in the *fused in sarcoma/translocated in liposarcoma (FUS/TLS)* gene have recently been identified as a cause of FALS. The FUS/TLS-immunoreactive inclusions are consistently found in cases of frontotemporal lobar degeneration with BIs; however, the association between ALS cases with BIs and FUS/TLS accumulation is not well understood. We used immunohistochemistry to analyze 3 autopsy cases of FALS with the *FUS/TLS* mutation and with BIs using anti-FUS/TLS antibodies. The disease durations were 1, 3, and 9 years. As the disease duration becomes longer, there were broader distributions of neuronal and glial FUS/TLS-immunoreactive inclusions. As early as 1 year after the onset, BIs, neuronal cytoplasmic inclusions and glial cytoplasmic inclusions were found in the substantia nigra in addition to the anterior horn of the spinal cord. Glial cytoplasmic inclusions are found earlier and in a wider distribution than neuronal cytoplasmic inclusions. The distribution of FUS/TLS-immunoreactive inclusions in FUS/TLS-mutated FALS with BIs was broader than that of BIs alone, suggesting that the pathogenetic mechanism may have originated from the FUS/TLS proteinopathy.

Key Words: Autopsy, Basophilic inclusions, Familial amyotrophic lateral sclerosis, Fused in sarcoma/translocated in liposarcoma.

From the Department of Neurology, Tohoku University School of Medicine, Sendai (N Suzuki, HW, HM, MK, N Shimakura, MA); Department of Brain and Neurosciences, Division of Neuropathology (SK), and Department of Microbiology and Pathology, Division of Molecular Pathology (MK), Tottori University Faculty of Medicine, Yonago; Department of Psychogeriatrics, Tokyo Institute of Psychiatry, Tokyo (HA, ZK); and Department of Neurology, Nishitaga National Hospital, Sendai (HK), Japan.

Send correspondence and reprint requests to: Naoki Suzuki, MD, PhD, Department of Neurology, Tohoku University School of Medicine, 1-1 Seiryo-machi, Aoba-ku, Sendai 980-8574, Japan; E-mail: naoki@med.tohoku.ac.jp

This work was supported by the following organizations and grants: Research on Measures for Intractable Diseases; Research on Psychiatric and Neurological Diseases and Mental Health from the Japanese Ministry of Health Labor and Welfare (Masashi Aoki and Shinsuke Kato); Grants-in-Aid for Scientific Research and Grants-in-Aid for Young Scientist (22790810, N Suzuki) from the Japanese Ministry of Education, Culture, Sports, Science and Technology; a grant (No. S0801035, Shinsuke Kato) from the Ministry of Education, Science, Sports and Culture of Japan; and Grants-in-Aid from the Research Committee of CNS Degenerative Diseases, the Ministry of Health, Labour and Welfare of Japan (Masashi Aoki and Shinsuke Kato).

INTRODUCTION

Amyotrophic lateral sclerosis (ALS) is an adult-onset neurodegenerative disorder characterized by the death of motor neurons (1). Autosomal-dominant familial cases account for nearly 10% of ALS cases. Approximately 10% to 20% of familial ALS (FALS) cases are caused by mutations in the *superoxide dismutase 1 (SOD1)* gene (1, 2). Mutations in the *TARDBP* gene, which codes for TAR DNA–binding protein 43 (TDP-43), have also been reported in FALS cases (3).

Recently, 2 groups reported that the autosomal dominant form of FALS is caused by mutations in the *fused in sarcoma/translocated in liposarcoma (FUS/TLS)* gene (4, 5), following several reports of both familial and sporadic cases from Europe (6–9) and Japan (10, 11). The FUS/TLS is a nucleoprotein that is involved in DNA and RNA metabolism (12). It binds to mRNA/DNA or other heterogeneous nuclear ribonucleoproteins through its C-terminus, regulating the splicing and transport of pre-mRNA; binding of its N-terminus to polymerases leads to transcriptional activation. Using an in vitro model, the nuclear localization signal in the C-terminus of FUS/TLS was found to be necessary for nuclear import (13–15).

Neuropathologic examination in FUS/TLS ALS cases has revealed severe lower motor neuron loss in the spinal cord and to a lesser degree in the brainstem as well as mild to moderate upper motor neuron loss in the motor cortex (10). Immunohistochemical staining of FUS/TLS within neuronal and non-neuronal nuclei is observed in both controls and patients with ALS, whereas additional promnent cytoplasmic FUS/TLS staining or elongated inclusions in spinal cord motor neurons and dystrophic neurites are found only in ALS patients. Subsequent studies have found FUS/TLS-immunoreactive (ir) neuronal cytoplasmic inclusions (NCIs) and glial cytoplasmic inclusions (GCIs) in tau-negative and TDP-43–negative frontotemporal lobar degeneration (FTLD), including atypical FTLD with ubiquitinated inclusions, neuronal intermediate filament inclusion disease, and basophilic inclusion (BI) body disease (16).

Munoz et al (16) reported the occurrence of FUS/TLS-ir NCIs, dystrophic neuritis, and GCIs in 2 cases of SALS with BIs that were previously reported by Kusaka et al (17). More recently, Tateishi et al (18) identified the R521C mutation in the *FUS/TLS* gene in FALS cases with BIs and found FUS/TLS-ir BIs and GCIs in affected areas. These findings suggest the possibility that BIs and FUS/TLS-ir structures are both

pathological hallmarks of a subset of FALS and SALS cases. We have also reported another Japanese FALS family with the R521C *FUS/TLS* mutation and BIs (11).

Here, we report a large Japanese FALS family with R521C mutations in the *FUS/TLS* gene with early disease onset. We performed pathological examinations on 3 autopsy cases with disease durations of 1, 3, or 9 years.

MATERIALS AND METHODS

ALS Cases

The family history revealed FALS in 23 of 46 family members (Fig. 1), suggesting a 100% penetrance rate (11). The average disease onset was at 35.3 ± 5.1 years (n = 12). The disease duration (from onset to respiratory failure) was 16.1 ± 7.7 months. The disease course was rapidly progressive, and the average age of death was 37.2 ± 4.2 years (n = 12). We did not find any cognitive impairment in the FALS patients with the *FUS/TLS* mutation in generations IV to VI of the family (Fig. 1).

Patient 1 was a man with an autosomal-dominant hereditary burden, as described in a previous report (11). At age 30 years, he developed muscle weakness in the distal part of his right upper extremity, followed by dysarthria, dysphagia, muscle weakness, and atrophy in all 4 extremities. Sensory, cerebellar, and higher cortical functions were not affected. At age 31 years, he required ventilatory support. He died of bronchopneumonia at age 40 years, that is, 9 years after disease onset.

Patient 2 was a woman described in a previous report, who suffered from FALS with posterior column degeneration and BIs (10, 19). At age 42 years, she developed muscle weakness in the proximal part of her upper extremities, followed by dysarthria, dysphagia, muscle weakness, and atrophy in her lower extremities. At age 44 years, she required ventilatory support. She died of bronchopneumonia at age 45 years, that is, her total disease duration was 3 years.

Patient 3 was a 48-year-old woman who started to notice muscle weakness in her right hand and muscle cramps in both legs. Five months later, she developed muscle weakness in all 4 limbs and subsequently noticed shortness of breath. Approximately 1 year after the onset of symptoms, she began to have difficulty in excreting sputum and developed dyspnea. She died of respiratory failure almost 1 year after the onset of her symptoms.

Genetic Examination

After written informed consent was obtained, DNA extraction and genotyping were performed using standard protocols, as previously described (11, 20). We sequenced all the exons from patient 1. The study was approved by the Ethics Committee (2009–384).

Neuropathologic Examination

Brain tissue samples were fixed postmortem with 10% formalin and embedded in paraffin, as previously described (5). Six-micrometer-thick tissue sections were prepared from the frontal, temporal, parietal, occipital, insular, and cingulate cortices, hippocampus, amygdala, basal ganglia, midbrain, pons, medulla oblongata, cerebellum, and the cervical, thoracic, lumbar, and sacral spinal cord. Deparaffinized sections were incubated for 30 minutes in 0.3% H_2O_2 to quench endogenous peroxidase activity and then washed with PBS. Sections were stained using the hematoxylin and eosin (H&E) and Klüver-Barrera (KB) methods. The severity of neuronal loss and tract degeneration was evaluated as none (−), mild (+), or severe (++). The presence of BIs was scored as absent (−), present (p), or prominently present (pp) (Table).

Rabbit polyclonal anti–TDP-43 (1:500; Protein Tech, Chicago, IL), rabbit polyclonal anti-ubiquitin (1:1000; Abcam, Cambridge, UK), and rabbit polyclonal anti-FUS/TLS (1:200, A300-302A; Bethyl, Montgomery, TX) antibodies were used. The reaction products were visualized with 3,3′-diaminobenzidine tetrahydrochloride, and hematoxylin was used to counterstain cell nuclei. The FUS/TLS-ir structures were assessed and

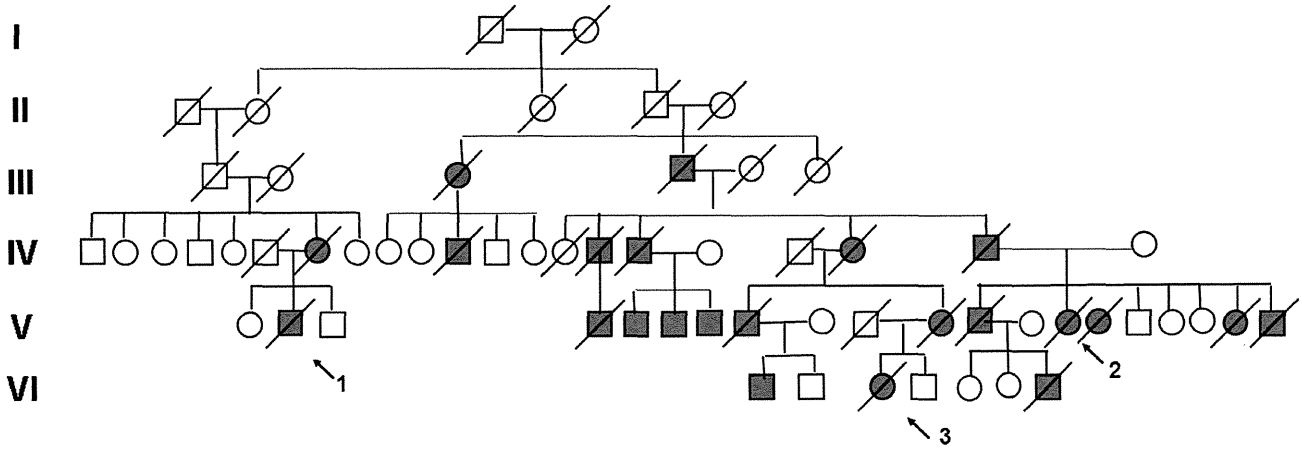

FIGURE 1. Pedigree of a Japanese family with familial amyotrophic lateral sclerosis and *FUS/TLS* mutations. Males are indicated by squares; females are indicated by circles. Affected members are indicated by solid symbols; deceased individuals are indicated by diagonals. Cases marked with numbers represent the autopsy cases. Generations are represented in Roman numerals.

TABLE. The Distribution and Severity of FUS/TLS-Immunoreactive Structures in CNS Regions

	FALS 1 year					FALS 3 years					FALS 9 years				
	DEG	BI	NCI	DN	GCI	DEG	BI	NCI	DN	GCI	DEG	BI	NCI	DN	GCI
Cerebrum															
Corpus callosum	N	N	N	N	N	−	N	N	N	−	−	N	N	N	+
Cingulate gyrus cortex	N	N	N	N	N	−	−	−	−	−	−	−	+	−	+
Cingulate white matter	N	N	N	N	N	−	N	N	N	−	−	N		N	+
Frontal cortex	−	−	−	−	−	−	−	+	−	+	−	p	++	++	++
Frontal white matter	−	N	N	N	−	−	N	N	N	−	−	N	N	N	+
Primary motor cortex	N	N	N	N	N	−	P	+	−	+	+	p	++	++	++
Primary motor white matter	N	N	N	N	N	−	N	N	N	+	−	N	N	N	+
Amygdala	N	N	N	N	N	−	−	−	−	−	N	N	N	N	N
Hippocampal dentate gyrus	−	−	−	−	−	−	−	−	−	−	−	−	−	−	−
Hippocampal CA	−	−	−	−	−	−	−	−	−	−	−	−	+	−	+
Subiculum	−	−	−	−	−	−	−	−	−	−	−	−	+	−	+
Temporal cortex	−	−	−	−	−	−	−	−	−	−	−	−	+	+	++
Temporal white matter	−	N	N	N	−	−	N	N	N	−	−	N	N	N	+
Caudate nucleus	−	−	−	−	−	−	−	−	−	−	−	−	+	++	++
Putamen	−	−	−	−	−	−	−	+	−	++	−	−	+	++	++
Globus pallidus	−	−	−	−	−	+	−	+++	++	++++	+	p	+++	+++	+++
Thalamus	−	−	−	−	−	−	−	+	−	+	−	−	+	++	++
Subthalamic nucleus	N	N	N	N	N	−	P	N	N	N	+	pp	+++	+++	++++
Meynert nucleus	N	N	N	N	N	−	−	−	−	+	−	−	+	+	++
Midbrain															
Substantia nigra	Min	p	+	−	+	+	P	++	+	+++	++	p	+++	+++	+++
Periaqueductal gray matter	N	N	N	N	N	−	P	+++	+	+	++	p	++++	+++	+++
Oculomotor nucleus	N	N	N	N	N	−	−	+	−	+	+	pp	+++	++	++
Trochlear nucleus	N	N	N	N	N	−	−	N	N	N	N	N	N	N	N
Reticular formation	N	N	N	N	N	N	−	+	+	++	+	−	++	++	++
Red nucleus	−	−	−	−	−	−	−	−	+	−	+	p	+++	+++	+++
Medial longitudinal fasciculus	−	N	N	N	−	−	N	N	N	N	+	N	N	N	++
Cerebral peduncle	−	N	N	N	−	−	N	N	N	+	+	N	N	N	+++
Pons															
Motor nucleus of trigeminal nerve	N	N	N	N	N	+	−	N	N	N	+	−	++	++	++
Locus coeruleus	−	−	+	−	−	−	p	+	−	−	+	p	+++	++	++
Reticular formation	−	−	−	−	−	N	N	++	++	+	+	−	++	++	++
Central tegmental tract	−	−	−	−	−	−	N	N	N	+	+	N	N	N	++
Superior cerebellar peduncle	−	−	−	−	−	−	N	N	N	−	+	N	N	N	+
Pontine nucleus	−	−	−	−	−	−	p	+	−	−	+	pp	++	++	++
Pyramidal tract	−	−	−	−	−	−	N	N	N	+	+	N	N	N	++
Medulla oblongata															
Hypoglossal nucleus	N	N	N	N	N	++	−	−	+	+	++	p	++	+	+
Dorsal vagal nucleus	N	N	N	N	N	−	−	+	−	−	+	−	++	++	++
Nucleus tractus solitarius	N	N	N	N	N	−	−	−	−	−	+	−	+	+	+
Gracile nucleus	N	N	N	N	N	+	p	N	N	N	+	p	++	++	++
Cuneate nucleus	N	N	N	N	N	++	p	++++	+	+	+	pp	+++	++	++
Spinal nucleus of trigeminal nerve	N	N	N	N	N	N	−	+	+	+	+	−	++	++	++
Inferior olivary nucleus	N	N	N	N	N	−	−	−	−	+	+	p	+++	+++	+++
Reticular formation	N	N	N	N	N	N	p	+++	++	+++	+	−	+	++	++
Medial lemniscus	N	N	N	N	N	−	N	N	N	+	+	N	N	N	+
Pyramid	N	N	N	N	N	−	N	N	N	+	++	N	N	N	++
Cerebellum															
Purkinje cells	+	−	−	−	−	+	−	−	−	−	++	−	−	−	−
Dentate nucleus	−	−	−	−	−	−	p	++	−	−	+	p	++	++	+++
White matter	−	−	−	−	−	−	N	N	N	−	++	N	N	N	+

(Continued on next page)

TABLE. The Distribution and Severity of FUS/TLS-Immunoreactive Structures in CNS Regions

	FALS 1 year					FALS 3 years					FALS 9 years				
	DEG	BI	NCI	DN	GCI	DEG	BI	NCI	DN	GCI	DEG	BI	NCI	DN	GCI
Spinal cord															
Anterior horn	++	p	++	++	++	++	p	++	+	+++	++	p	+	+	+
Posterior horn	−	−	−	−	−	N	−	+	N	+	+	−	+	+	+
Clarke nucleus	−	−	−	−	−	+	−	−	−	−	++	−	+	+	+
Intermediolateral horn	−	−	−	−	−	−	−	−	−	−	+	−	−	+	+
Anterior and lateral CST	Min	N	N	N	+	+	N	N	N	+	++	N	N	N	++
Anterior and lateral funiculi	+	N	N	N	+	++	N	N	N	++	++	N	N	N	+
Gracile fasciculus	−	N	N	N	−	+	N	N	N	−	++	N	N	N	++
Cuneate fasciculus	−	N	N	N	+	++	N	N	N	−	++	N	N	N	+
Middle root zone	Min	N	N	N	−	+	N	N	N	N	++	N	N	N	++

FUS/TLS neuronal and glial inclusions were scored as none (−), rare (+), occasional (++), common (+++), or numerous (++++). Degeneration was scored as none (−), mild (+), or severe (++). The BIs were scored as absent (−), present (p), or prominently present (pp).

BI, basophilic inclusion; CST, corticospinal tract; DD, disease duration; DEG, degeneration assessed in H&E- and Klüver-Barrera–stained sections; DN, FALS 1 year, patient 3; FALS 3 years, patient 2; FALS 9 years, patient 1; FUS/TLS-immunoreactive dystrophic neurites; GCI, FUS/TLS-immunoreactive glial cytoplasmic inclusion; Min, minimal change; N, not evaluated (or unable to evaluate); NCI, FUS/TLS-immunoreactive neuronal cytoplasmic inclusion.

scored as none (−), rare (+), occasional (++), common (+++), or numerous (++++), as previously described (10) (Table).

RESULTS

Mutation Analysis

We detected a missense mutation (*c.1561C→T*) in the *FUS/TLS* gene that substituted cysteine for arginine at residue 521 (R521C) in patient 1 (11). A sequence analysis of the FUS/TLS gene in patients 2 and 3 could not be performed because only formalin-fixed and paraffin-embedded tissues were available. Identification of the R521C FUS/TLS mutation in patient 1 suggests that patients 2 and 3 likely carried the same FUS/TLS mutation.

Neuropathologic Findings

The distribution and severity of neuronal degeneration, BIs, and FUS/TLS-ir structures across CNS regions are summarized in the Table.

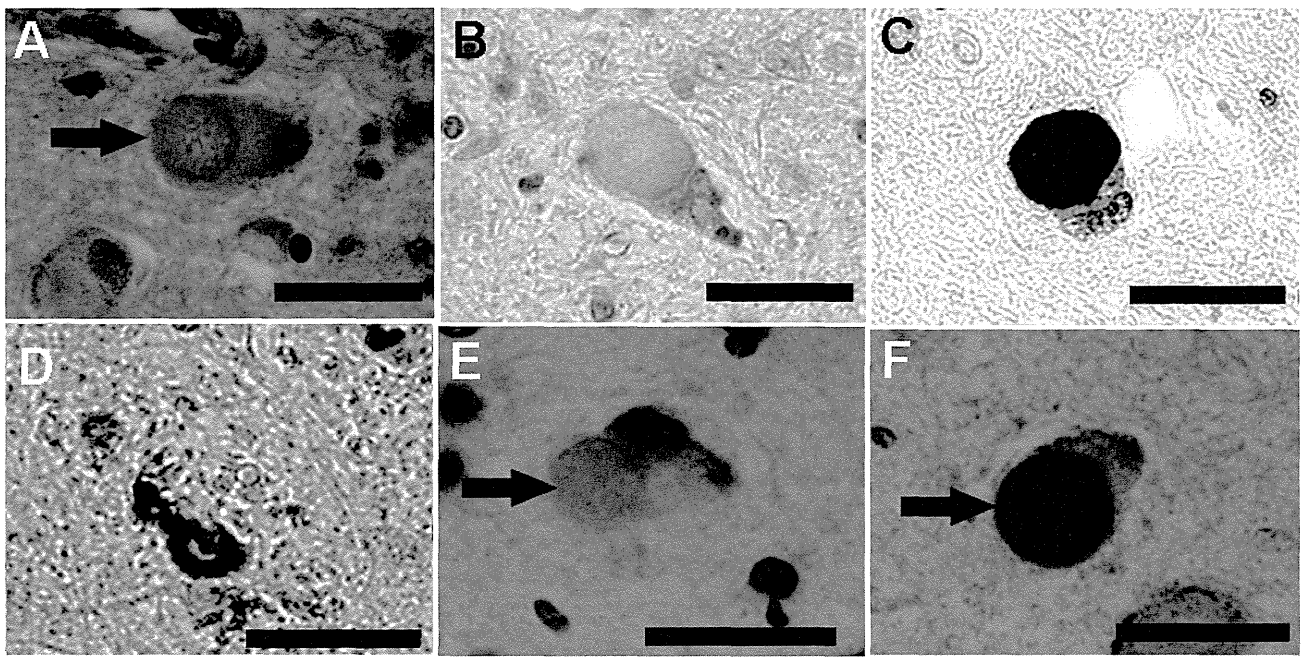

FIGURE 2. Pathological features of patient 1. (**A**) Hematoxylin and eosin staining. There are a few BI bodies in the neurons of the brainstem (arrow). (**B**) Klüver-Barrera stain reveals an inclusion in the cytoplasm of a neuron. (**D–F**) Numerous FUS/TLS-immunoreactive inclusions are found in brainstem neurons (**C**) and glial cells (**D**). These inclusions were immunostained with ubiquitin (**F**, arrow) but not with TDP-43 (**E**, arrow). Scale bar = 30 μm.

Examination of patient 1 revealed neuronal loss in the upper and lower motor neuron systems and Clarke column and degeneration of the pyramidal tracts, the middle root zone of the posterior column, and the posterior spinocerebellar tract. Atrophy of the brainstem tegmentum was remarkable. There was marked neuronal loss in the anterior horn of the spinal cord. Neuronal loss was also noted in the substantia nigra, globus pallidus, periaqueductal gray matter, oculomotor nucleus, reticular formation of the brainstem, red nucleus, cerebral peduncle, motor nucleus of the trigeminal nerve, locus coeruleus, central tegmental tract, pontine nucleus, hypoglossal nucleus, and the gracile nucleus. Betz cells were sparse in the primary motor cortex versus the primary cortices of normal controls. Along the entire spinal cord, the anterior and lateral funiculi, including the spinothalamic and spinocerebellar tracts, were extensively degenerated. The BIs were observed in H&E- and KB-stained sections and were detected in Betz cells, the globus pallidus, subthalamic nucleus, substantia nigra, red nucleus, periaqueductal gray matter, locus coeruleus, oculomotor nucleus, pontine nucleus, lateral cuneate nucleus, gracile nucleus, reticular formation of the medulla oblongata, cerebellar dentate nucleus, and anterior horn of the lumbar cord (Fig. 2A, B) (11). Most BIs were homogeneous and round without a halo or core, as previously reported (21). The color of the BIs in the H&E-stained sections was closer to pink than blue, with occasional thin basophilic rims, which is consistent with some previous descriptions (22). The basophilic bodies were ubiquitin ir (Fig. 2F), but not TDP-43 ir (Fig. 2E) (11). Numerous FUS/TLS-ir inclusions were found in neurons and glial cells (Fig. 2C, D).

Examination of patient 2 has been previously described (10, 19) and is summarized in the Table. The distribution of degeneration was not as broad as in patient 1. Degeneration was observed in the primary motor cortex, subthalamic nucleus, periaqueductal gray matter, red nucleus, medial longitudinal fasciculus, cerebral peduncle, locus coeruleus, superior cerebellar peduncle, pontine nucleus, dorsal vagal nucleus, nucleus tractus solitarius, inferior olivary nucleus, medial lemniscus, dentate nucleus, cerebellar white matter, and Clarke nucleus. We found BIs in the primary motor cortex, subthalamic nucleus, substantia nigra, periaqueductal gray matter, locus coeruleus, pontine nucleus, gracile nucleus, cuneate nucleus, reticular formation, dentate nucleus, and the anterior horn (Table). In addition, there were NCIs and GCIs in the frontal white matter, putamen, globus pallidus, thalamus, oculomotor nucleus, reticular formation, and the posterior horn.

In patient 3, KB staining showed severe loss of anterior horn neurons compared with a control (Fig. 3A, B). The BIs were observed in both H&E (Fig. 3C)- and KB-stained sections (Fig. 3D). The FUS/TLS-ir cytoplasmic inclusions were present in surviving motor neurons (Fig. 3E). Glial cells with FUS/TLS-ir cytoplasmic inclusions appeared to be oligodendroglia (Fig. 3F). Degeneration was only found in the anterior horn, substantia nigra, corticospinal tract, and the middle root zone. The BIs were only present in the substantia nigra and anterior horn of the spinal cord (Table). The NCIs were found in the substantia nigra, locus coeruleus, and the anterior horn of the spinal cord. The GCIs were also found in the substantia nigra, anterior horn, corticospinal tract, and cuneate fasciculus of the spinal cord (Table).

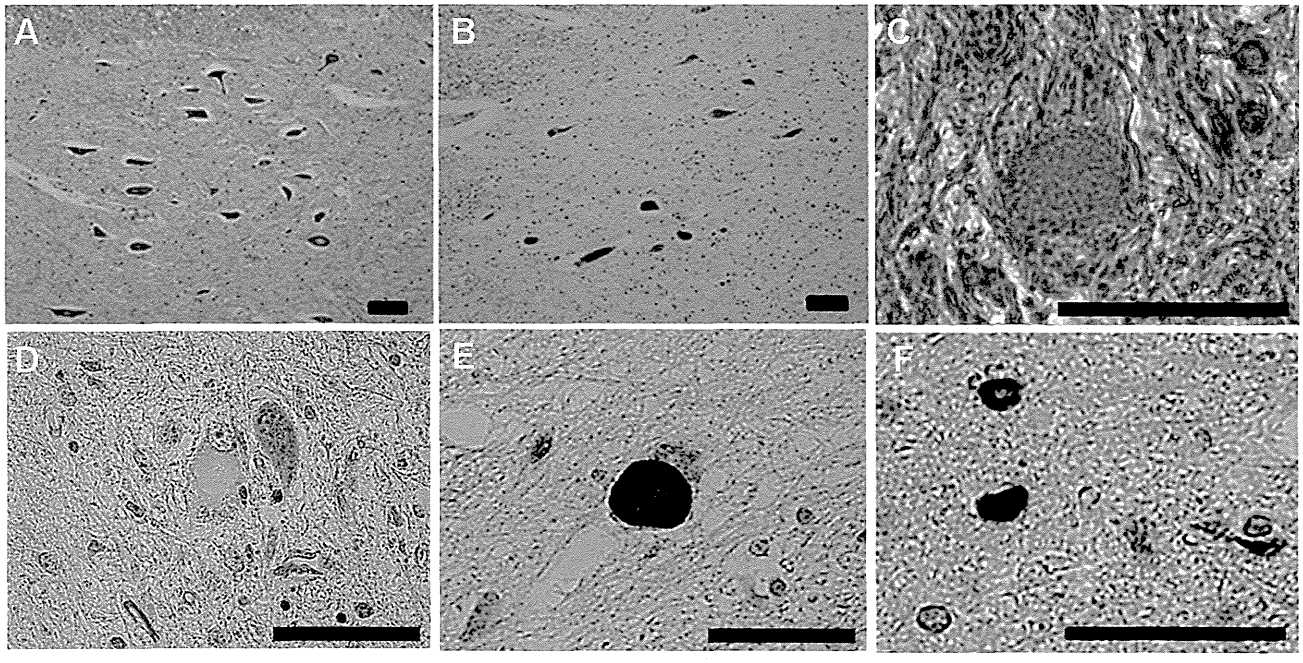

FIGURE 3. Pathological features of patient 3. (**A–D**) Klüver-Barrera staining (**A, B, D**) shows a marked loss of anterior horn neurons (**B**) in patient 3 compared with an age-matched control (**A**). A BI was also found (**D**). A BI was also observed with hematoxylin and eosin staining (**C**). (**E, F**) The FUS/TLS-positive cytoplasmic inclusions are present in a surviving motor neurons (**E**) and in glial cells with a FUS/TLS-positive cytoplasmic inclusion (**F**). Scale bar = 50 μm.

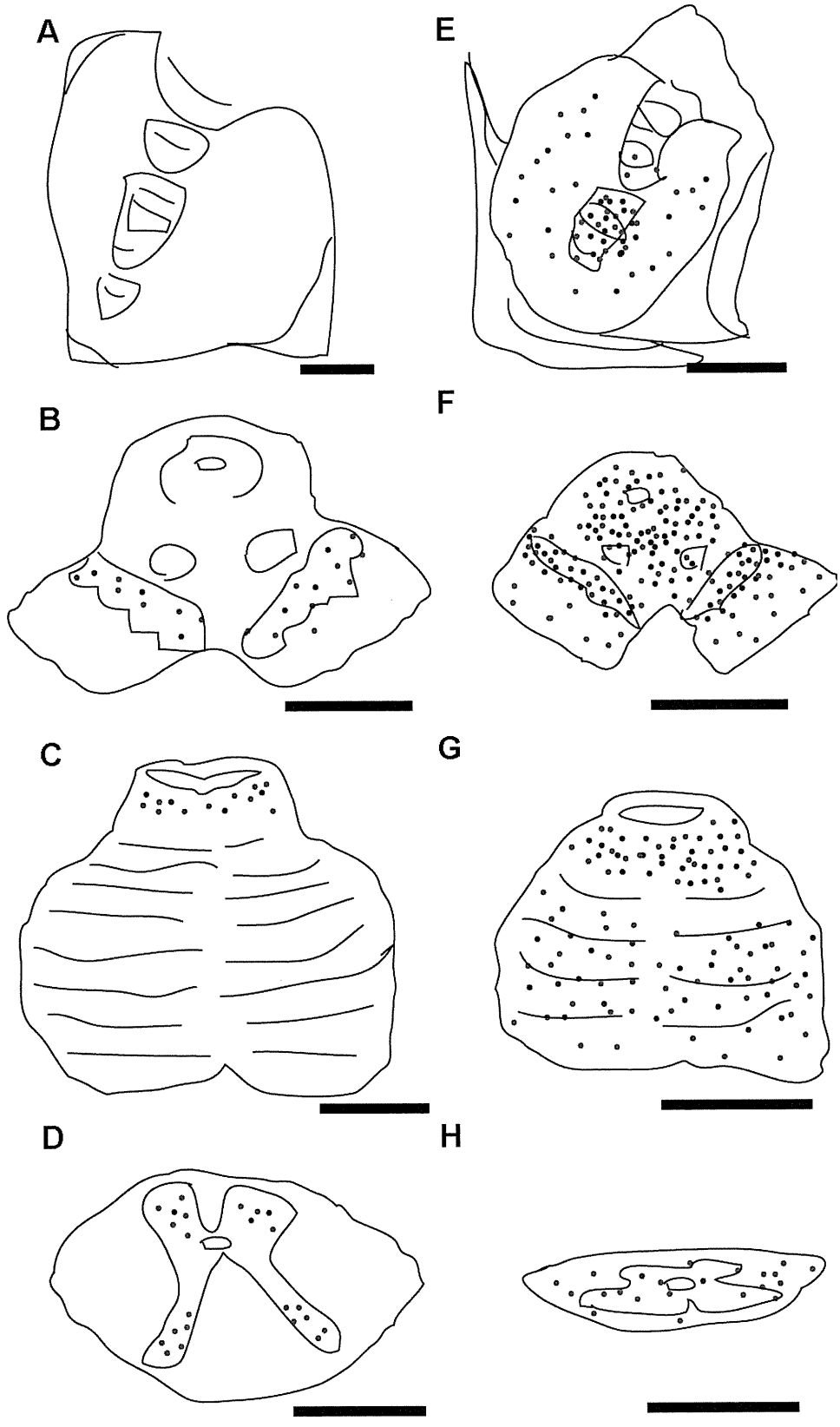

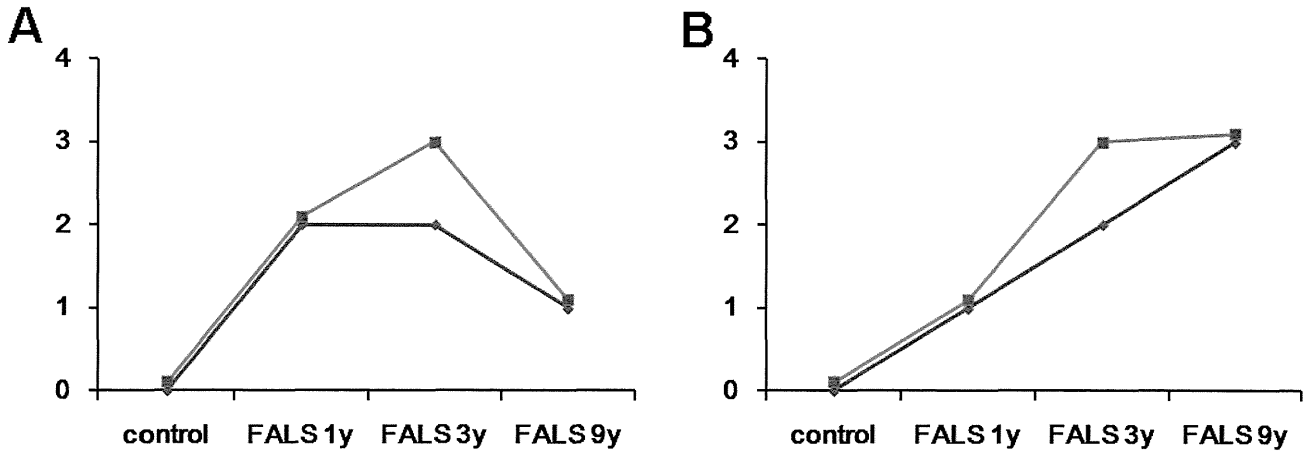

FIGURE 5. The FUS/TLS-immunoreactive inclusions were counted and represented semiquantitatively as follows: no more than 1 (n = 0); rare (n = 1); occasional (n = 2); common (n = 3); or numerous (n = 4). (**A, B**) The anterior horn (**A**) and substantia nigra (**B**) were examined. Glial cytoplasmic inclusions (GCIs) are indicated as a blue line; neuronal cytoplasmic inclusions (NCIs) are indicated as a red line. The horizontal axis represents the duration of disease: control; familial ALS (FALS) 1 year, patient 3; FALS 3 years, patient 2; FALS 9 years, patient 1.

The FUS/TLS-ir inclusions were distributed more widely with longer disease durations. Figure 4 illustrates inclusions in the basal ganglia (Fig. 4A, E), midbrain (Fig. 4B, F), upper pons (Fig. 4 C, G), and cervical spinal cord (Fig. 4D, H) in patient 3 (Fig. 4A–D) and patient 1 (Fig. 4E–H). The FUS/TLS-ir inclusions were counted and are represented semiquantitatively in the anterior horn and substantia nigra, respectively (Fig. 5A, B); however, we were not able to evaluate them thoroughly. With respect to NCIs, the anterior horn cells were severely degenerated, and many NCIs were found in the anterior horn cells even in patients 2 and 3. Most of the neurons that disappeared in patient 1 resulted in decreased numbers of NCIs; thus, the decrease in NCIs in the anterior horn resulted from the loss of anterior horn cells. In contrast, we detected an increase in the number of NCIs in the substantia nigra in the case with long (9 years) versus short (1 year) duration. There were numerous GCIs in the anterior horn in patient 2 and fewer GCIs in patient 1. In the substantia nigra, the number of GCIs was also greater in the case of long versus short duration. The apparent early appearance of FUS/TLS-ir inclusions and severe degeneration in the terminal stage in the anterior horn indicated that the motor neuron system was the most severely affected region in FUS/TLS-mutated FALS, although multiple systems were involved in the advanced disease.

DISCUSSION

Recent work suggests a new biochemical category of neurodegenerative diseases in terms of the aberrant accumulation of FUS/TLS (FUS/TLS proteinopathy). The *FUS/TLS* mutations have been found in 3% to 5% of patients with FALS (4, 5, 8, 9, 23) and in some SALS cases (7, 24). The R521C mutation is one of the most common. As reported previously in cases with this type of mutation, weakness of the neck and/or proximal upper limbs is frequently observed, and bulbar dysfunction, dystonia, or frontotemporal dementia are rarely observed; there is no sensory disturbance, ataxia, or parkinsonism. The clinical features of the present cases are largely consistent with those previously reported. To date, 6 papers have described the neuropathology of patients with the R521C mutation (4, 5, 10, 18, 25, 26), but this study is the first to describe temporally serial pathological examinations in affected family members that presumably had the same mutation. Recently, Neumann et al (27) reported that the FET proteins TAF15 and EWS are selective markers that distinguish FTLD with FUS/TLS pathology from ALS with the FUS/TLS mutation. In this series, however, none of the 3 cases had cognitive impairment.

Although the marked loss of NCIs in patient 1 may be caused by the long disease duration and the use of artificial ventilation and not because of the FUS/TLS mutation itself, this is the first report of serial autopsied FALS cases with BIs in the same family showing a widespread occurrence of FUS/TLS-ir neuronal and glial inclusions. Patients in this family likely had the same mutation as patient 1 based on the autosomal-dominant trait pattern (Fig. 1).

It is noteworthy that the distributions of FUS/TLS-ir structures and degeneration occurred largely in parallel in the cerebrospinal regions (Table). Aberrant accumulation of FUS/TLS plays an important role in degeneration. In patient 3, prominent neuronal degeneration was found in the anterior

FIGURE 4. The FUS/TLS-immunoreactive inclusions are distributed widely in the CNS as the disease progresses. (**A–H**) Illustrations depict basal ganglia (**A, E**), midbrain (**B, F**), pons (**C, G**), and cervical spinal cord (**D, H**) in tissues from patient 3 (1 year after onset, **A–D**) and patient 1 (9 years after onset, **E–H**). Blue circles represent neuronal FUS/TLS-immunoreactive inclusions; red circles represent glial FUS/TLS-immunoreactive inclusions. Scale bars = (**A–C, E, F**) 1 cm; (**D, G, H**) 0.5 cm.

horn of the spinal cord and only extended to the substantia nigra. As we observed in the relatively earlier stages of ALS, there is multisystem degeneration despite the fact that clinical manifestations are restricted to the motor system. The middle root zone of the spinal cord had degenerated even in the early disease stage in patient 3. Although the middle root zone had degenerated in an SOD1-mutated ALS patient (28), it was also the characteristic finding in *FUS/TLS*-mutated ALS patients. Before the identification of the *FUS/TLS* mutation as the cause for the disease, FALS with BIs was described in some reports (17, 19, 29, 30). From our extensive survey, we found broader distributions of FUS/TLS-ir structures than those of BIs, suggesting that degeneration beyond the motor neuron system had occurred in our patients even in the early stages of

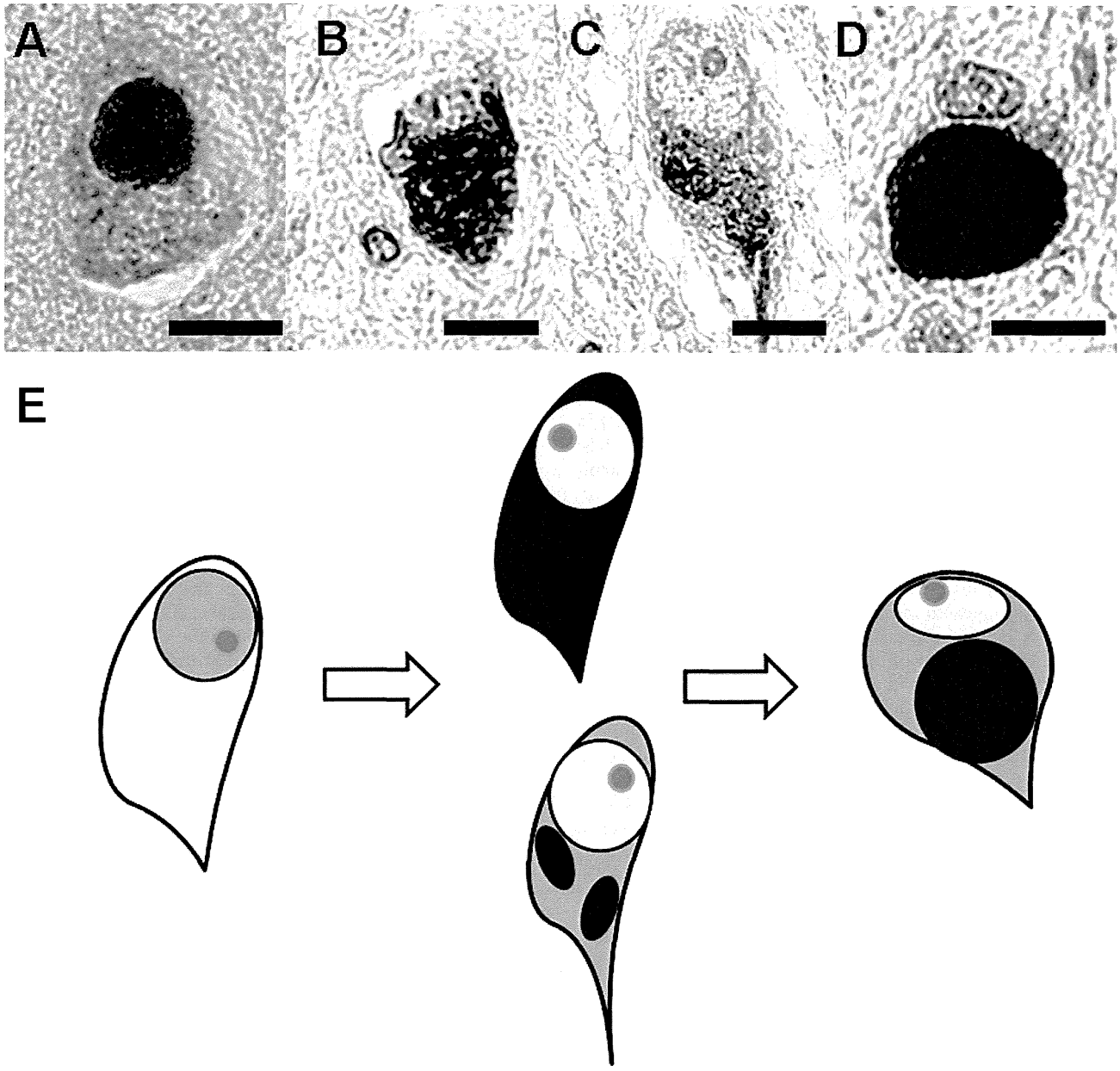

FIGURE 6. The range of FUS/TLS-immunoreactive neurons observed in patient 1. (**A**–**D**) There were morphologically normal neurons (**A**), early FUS/TLS redistribution, loss of staining in nuclei and predominantly cytoplasmic staining (**B**), staining of cytoplasmic aggregates (**C**), and the later occurrence of a cytoplasmic FUS/TLS-immunoreactive inclusion in an atrophic neuron (**D**). Scale bar = 50 μm. (**E**) Hypothetical model of the progression of FUS/TLS pathology. Normal distribution of FUS/TLS in the nucleus (left), increased distribution of FUS/TLS in the cytoplasm and exclusion from the nucleus (middle), and larger inclusions in the cytoplasm (right) appear as the disease progresses.

the disease. On the other hand, in some respirator-assisted patients with sporadic ALS who survived long-term, the degeneration did not extend beyond the upper and lower motor neurons (28, 31). In addition, in 2 patients with long-term sporadic ALS without respirator support (1 with a 9-year history and the other with an 11-year history), the pathological findings were similar to those of typical classical ALS (28). This suggests that the multisystem degeneration of our autopsy cases does not seem to be simply attributable to the long-term survival assisted by ventilator support.

Pathogenetic mechanisms of *FUS/TLS*-mutated ALS have not been elucidated. Glial cells carrying a human *SOD1* mutation have a direct non-cell autonomous effect on motor neuron survival (32, 33). Whether the aberrant expression of FUS/TLS in glial cells also has a non-cell autonomous effect on motor neuron survival has not yet been examined. Here, we provide spatial and semiquantitative data on NCIs and GCIs in the spinal cord and substantia nigra (Figs. 4, 5). With respect to NCIs, the anterior horn cells were severely degenerated and contained many NCIs even in patients 2 and 3. Most of the neurons that disappeared in patient 1 resulted in decreased numbers of NCIs, indicating that the decrease in NCIs was caused by the loss of anterior horn cells. In contrast, we detected increasing numbers of NCIs in the substantia nigra in the case of 9-year duration. We found many GCIs in the anterior horn in patient 2 and fewer in patient 1. In patient 2, we observed the pathology of ongoing neuronal degeneration, and GCIs were more prominent than NCIs in both the anterior horn and the substantia nigra. Thus, the GCIs appeared to be prominent in a transition period, that is, the middle disease duration of patient 2. Similar to pathogenesis of *SOD1*-mutated FALS, the non-cell autonomous effects of glial cells may influence the progression of FUS/TLS proteinopathy. In contrast, it has previously been reported that alsin-depleted ALS spinal motor neurons can be rescued from defective survival and axon growth through coculture with astrocytes in vitro (34). It is possible that glial cells have a protective role by promoting the clearance of mutated FUS/TLS proteins from FUS/TLS-ir inclusions in neurons. The TDP-43 is detected in the spinal fluid of ALS patients (35), which may indicate that FUS/TLS (which contains similar functional domains as TDP-43) may be excreted from neuronal cells and might be processed by glial cells. The role of glial cells carrying *FUS/TLS* mutation remains unclear.

There are various types of FUS/TLS-ir neurons. We observed several types of FUS/TLS-ir structures in patient 1 (Fig. 6A–D). In patient 3, the frequency of NCI (Fig. 6D) was not very high, and most neuronal cells showed a nuclear FUS/TLS staining pattern. Because the nuclear localization signal in the C-terminus of FUS/TLS was found to be necessary for nuclear import (13, 14, 15), we propose that there is progression of the cytopathology of FUS/TLS proteinopathy such that 1) morphologically normal neurons have FUS/TLS-ir in the nucleus (Fig. 6 A); 2) there is the early occurrence of FUS/TLS redistribution, including low expression in the nucleus and high expression in the cytoplasm (Fig. 6B); 3) this is followed by loss of staining in the nucleus with predominantly cytoplasmic staining (Fig. 6C); and 4) cytoplasmic FUS/TLS aggregates are found in atrophic neurons (Fig. 6D). These observations may parallel the production of NCIs in FUS/TLS-mutant transgenic cell models (14).

There are many similarities between FUS/TLS and TDP-43. They are both DNA/RNA-binding proteins involved in transcriptional regulation, mRNA splicing, transport, and translation (36). Mutations in both genes cause ALS (16), and both gene products accumulate in neurons and glial cells. In our patient with the R521C *FUS/TLS* mutation, TDP-43 had a normal distribution. Regardless of their functional similarities, FUS/TLS and TDP-43 may contribute to the development of ALS by distinct molecular pathways. The messenger RNA or microRNA of these autopsy cases should be examined.

Recently, Huang et al (37) reported that FUS/TLS transgenic rats develop ALS and FTLD phenotypes. Mutant FUS/TLS transgenic rats developed progressive paralysis secondary to the degeneration of motor axons and displayed a substantial loss of neurons in the cortex and hippocampus. Even transgenic rats that overexpressed the wild-type human FUS/TLS showed a deficit in spatial learning and memory and a significant loss of cortical and hippocampal neurons at advanced ages. A disease model using a knock-in system or a cell-specific mutant would be necessary to support our hypothesis on the mechanisms of the progression scenario that we hypothesize.

In conclusion, we have demonstrated a widespread occurrence of FUS/TLS-ir neuronal and glial structures in R521C-*FUS/TLS*–mutated FALS with BIs. Further studies using animal models are needed to examine the pathogenetic mechanisms of FALS-FUS/TLS.

ACKNOWLEDGMENT

The authors thank R. Ando and Y. Takahashi for their technical assistance. The authors also thank Mr Brent Bell for reading the manuscript.

REFERENCES

1. Pasinelli P, Brown RH. Molecular biology of amyotrophic lateral sclerosis: Insights from genetics. Nat Rev Neurosci 2006;7:710–23
2. Rosen DR, Siddique T, Patterson D, et al. Mutations in *Cu/Zn superoxide dismutase* gene are associated with familial amyotrophic lateral sclerosis. Nature 1993;362:59–62
3. Kabashi E, Valdmanis PN, Dion P, et al. TARDBP mutations in individuals with sporadic and familial amyotrophic lateral sclerosis. Nat Genet 2008;40:572–4
4. Vance C, Rogelj B, Hortobagyi T, et al. Mutations in FUS, an RNA processing protein, cause familial amyotrophic lateral sclerosis type 6. Science 2009;323:1208–11
5. Kwiatkowski TJ Jr, Bosco DA, Leclerc AL, et al. Mutations in the *FUS/TLS* gene on chromosome 16 cause familial amyotrophic lateral sclerosis. Science 2009;323:1205–8
6. Talbot K. Another gene for ALS: Mutations in sporadic cases and the rare variant hypothesis. Neurology 2009;73:1172–3
7. Belzil VV, Valdmanis PN, Dion PA, et al. Mutations in FUS cause FALS and SALS in French and French Canadian populations. Neurology 2009;73:1176–9
8. Chio A, Restagno G, Brunetti M, et al. Two Italian kindreds with familial amyotrophic lateral sclerosis due to FUS mutation. Neurobiol Aging 2009;30:1272–5
9. Corrado L, Del Bo R, Castellotti B, et al. Mutations of *FUS* gene in sporadic amyotrophic lateral sclerosis. J Med Genet 2010;47:190–4
10. Kobayashi Z, Tsuchiya K, Arai T, et al. Occurrence of basophilic inclusions and FUS-immunoreactive neuronal and glial inclusions in a case of familial amyotrophic lateral sclerosis. J Neurol Sci 2010;293:6–11

11. Suzuki N, Aoki M, Warita H, et al. FALS with FUS mutation in Japan, with early onset, rapid progress and basophilic inclusion. J Hum Genet 2010;55:252–4
12. Wang X, Arai S, Song X, et al. Induced ncRNAs allosterically modify RNA-binding proteins in cis to inhibit transcription. Nature 2008;454: 126–30
13. Ito D, Seki M, Tsunoda Y, et al. Nuclear transport impairment of amyotrophic lateral sclerosis-linked mutations in FUS/TLS. Ann Neurol 2011;69:152–62
14. Dormann D, Rodde R, Edbauer D, et al. ALS-associated fused in sarcoma (FUS) mutations disrupt Transportin-mediated nuclear import. EMBO J 2010;29:2841–57
15. Kino Y, Washizu C, Aquilanti E, et al. Intracellular localization and splicing regulation of FUS/TLS are variably affected by amyotrophic lateral sclerosis-linked mutations. Nucleic Acids Res 2011;39:2781–98
16. Munoz DG, Neumann M, Kusaka H, et al. FUS pathology in basophilic inclusion body disease. Acta Neuropathol 2009;118:617–27
17. Kusaka H, Matsumoto S, Imai T. An adult-onset case of sporadic motor neuron disease with basophilic inclusions. Acta Neuropathol 1990;80: 660–5
18. Tateishi T, Hokonohara T, Yamasaki R, et al. Multiple system degeneration with basophilic inclusions in Japanese ALS patients with FUS mutation. Acta Neuropathol 2010;119:355–64
19. Tsuchiya K, Matsunaga T, Aoki M, et al. Familial amyotrophic lateral sclerosis with posterior column degeneration and basophilic inclusion bodies: A clinical, genetic and pathological study. Clin Neuropathol 2001;20:53–9
20. Aoki M, Lin CL, Rothstein JD, et al. Mutations in the glutamate transporter *EAAT2* gene do not cause abnormal EAAT2 transcripts in amyotrophic lateral sclerosis. Ann Neurol 1998;43:645–53
21. Kusaka H, Matsumoto S, Imai T. Adult-onset motor neuron disease with basophilic intraneuronal inclusion bodies. Clin Neuropathol 1993;12: 215–8
22. Yokota O, Tsuchiya K, Terada S, et al. Basophilic inclusion body disease and neuronal intermediate filament inclusion disease: A comparative clinicopathological study. Acta Neuropathol 2008;115:561–75
23. Ticozzi N, Silani V, LeClerc AL, et al. Analysis of *FUS* gene mutation in familial amyotrophic lateral sclerosis within an Italian cohort. Neurology 2009;73:1180–5
24. Drepper C, Herrmann T, Wessig C, et al. C-terminal FUS/TLS mutations in familial and sporadic ALS in Germany. Neurobiol Aging 2011; 32:548.e1–4
25. Blair IP, Williams KL, Warraich ST, et al. FUS mutations in amyotrophic lateral sclerosis: Clinical, pathological, neurophysiological and genetic analysis. J Neurol Neurosurg Psychiatry 2010;81:639–45
26. Yamamoto-Watanabe Y, Watanabe M, Okamoto K, et al. A Japanese ALS6 family with mutation R521C in the *FUS/TLS* gene: A clinical, pathological and genetic report. J Neurol Sci 2010;296:59–63
27. Neumann M, Bentmann E, Dormann D, et al. FET proteins TAF15 and EWS are selective markers that distinguish FTLD with FUS pathology from amyotrophic lateral sclerosis with FUS mutations. Brain 2011;134: 2595–609
28. Kato S, Shimoda M, Watanabe Y, et al. Familial amyotrophic lateral sclerosis with a two base pair deletion in superoxide dismutase 1: Gene multisystem degeneration with intracytoplasmic hyaline inclusions in astrocytes. J Neuropathol Exp Neurol 1996;55:1089–101
29. Ito H, Kusaka H, Matsumoto S, et al. Topographic involvement of the striatal efferents in basal ganglia of patients with adult-onset motor neuron disease with basophilic inclusions. Acta Neuropathol 1995;89: 513–8
30. Matsumoto S, Kusaka H, Murakami N, et al. Basophilic inclusions in sporadic juvenile amyotrophic lateral sclerosis: An immunocytochemical and ultrastructural study. Acta Neuropathol 1992;83:579–83
31. Kato S, Oda M, Tanabe H. Diminution of dopaminergic neurons in the substantia nigra of sporadic amyotrophic lateral sclerosis. Neuropathol Appl Neurobiol 1993;19:300–4
32. Di Giorgio FP, Carrasco MA, Siao MC, et al. Non-cell autonomous effect of glia on motor neurons in an embryonic stem cell–based ALS model. Nat Neurosci 2007;10:608–14
33. Nagai M, Re DB, Nagata T, et al. Astrocytes expressing ALS-linked mutated SOD1 release factors selectively toxic to motor neurons. Nat Neurosci 2007;10:615–22
34. Jacquier A, Bellouze S, Blanchard S, et al. Astrocytic protection of spinal motor neurons but not cortical neurons against loss of Als2/alsin function. Hum Mol Genet 2009;18:2127–39
35. Kasai T, Tokuda T, Ishigami N, et al. Increased TDP-43 protein in cerebrospinal fluid of patients with amyotrophic lateral sclerosis. Acta Neuropathol 2009;117:55–62
36. Neumann M, Rademakers R, Roeber S, et al. A new subtype of frontotemporal lobar degeneration with FUS pathology. Brain 2009;132: 2922–31
37. Huang C, Zhou H, Tong J, et al. FUS transgenic rats develop the phenotypes of amyotrophic lateral sclerosis and frontotemporal lobar degeneration. PLoS Genet 2011;7:e1002011

Human Reproduction, Vol.27, No.8 pp. 2541–2548, 2012
Advanced Access publication on June 6, 2012 doi:10.1093/humrep/des197

human reproduction ORIGINAL ARTICLE *Reproductive genetics*

Characterization of DNA methylation errors in patients with imprinting disorders conceived by assisted reproduction technologies

Hitoshi Hiura[1], Hiroaki Okae[1], Naoko Miyauchi[1], Fumi Sato[1], Akiko Sato[1], Mathew Van De Pette[2], Rosalind M John[2], Masayo Kagami[3], Kunihiko Nakai[4], Hidenobu Soejima[5], Tsutomu Ogata[6], and Takahiro Arima[1,*]

[1]Department of Informative Genetics, Environment and Genome Research Center, Tohoku University Graduate School of Medicine, 2-1 Seiryo-cho, Aoba-ku, Sendai 980-8575, Japan [2]Cardiff School of Biosciences, Museum Avenue, Cardiff CF10 3US, UK [3]Division of Clinical Genetics and Molecular Medicine, National Center for Child Health and Development, 2-10-1 Okura, Seatagaya-ku, Tokyo 157-8535, Japan [4]Department of Development and Environmental Medicine, Tohoku University Graduate School of Medicine, Sendai 980-8575, Japan [5]Division of Molecular Genetics and Epigenetics, Department of Biomolecular Sciences, Faculty of Medicine, Saga University, Saga 849-8501, Japan [6]Department of Pediatrics, Faculty of Medicine, Hamamatsu University, Hamamatsu 431-3192, Japan

*Correspondence address. Tel: +81-22-717-7844; Fax: +81 22-717-7063; E-mail: tarima@med.tohoku.ac.jp

Submitted on February 9, 2012; resubmitted on March 29, 2012; accepted on May 1, 2012

BACKGROUND: There is an increased incidence of rare imprinting disorders associated with assisted reproduction technologies (ARTs). The identification of epigenetic changes at imprinted loci in ART infants has led to the suggestion that the techniques themselves may predispose embryos to acquire imprinting errors and diseases. However, it is still unknown at what point(s) these imprinting errors arise, or the risk factors.

METHODS: In 2009 we conducted a Japanese nationwide epidemiological study of four well-known imprinting diseases to determine any association with ART. Using bisulfite sequencing, we examine the DNA methylation status of 22 gametic differentially methylated regions (gDMRs) located within the known imprinted loci in patients with Beckwith-Wiedemann syndrome (BWS, $n = 1$) and also Silver-Russell syndrome (SRS, $n = 5$) born after ART, and compared these with patients conceived naturally.

RESULTS: We found a 10-fold increased frequency of BWS and SRS associated with ART. The majority of ART cases showed aberrant DNA methylation patterns at multiple imprinted loci both maternal and paternal gDMRs (5/6), with both hyper- and hypomethylation events (5/6) and also mosaic methylation errors (5/6). Although our study may have been limited by a small sample number, the fact that many of the changes were mosaic suggested that they occurred after fertilization. In contrast, few of the patients who were conceived naturally exhibited a similar pattern of mosaic alterations. The differences in methylation patterns between the patients who were conceived naturally or after ART did not manifest due to the differences in the disease phenotypes in these imprinting disorders.

CONCLUSION: A possible association between ART and BWS/SRS was found, and we observed a more widespread disruption of genomic imprints after ART. The increased frequency of imprinting disorders after ART is perhaps not surprising given the major epigenetic events that take place during early development at a time when the epigenome is most vulnerable.

Key words: assisted reproduction technologies / genomic imprinting / DNA methylation / gametic differentially methylated regions / genomic imprinting disorders

Introduction

Human assisted reproduction technologies (ARTs) are used in the treatment of infertility and involve the manipulation of eggs and/or sperm in the laboratory. Several recent studies have identified an increased incidence of some normally very rare imprinting disorders after ART, including Beckwith-Wiedemann syndrome (BWS: ONIM 130650), Angelman syndrome (AS: ONIM 105830) and Silver-Russell syndrome (SRS: OMIM 180860) but not Prader-Willi syndrome (PWS: OMIM 176270; DeBaun *et al.*, 2003; Gosden *et al.*, 2003; Svensson *et al.*, 2005). Additionally, there are several reports suggesting that epigenetic alterations (epimutations) at imprinted loci occur during the *in vitro* manipulation of the gametes, with both IVF and ICSI approaches implicated (Cox *et al.*, 2002; DeBaun *et al.*, 2003; Gicquel *et al.*, 2003; Maher *et al.*, 2003; Moll *et al.*, 2003; Orstavik *et al.*, 2003; Ludwig *et al.*, 2005; Rossignol *et al.*, 2006; Bowdin *et al.*, 2007; Kagami *et al.*, 2007). However, some studies do not support a link between ART and imprinting disorders (Lidegaard *et al.*, 2005; Doornbos *et al.*, 2007).

Epigenetic marks laid down in the male or female germ lines, and which are inherited by the embryos, establish the imprinted expression of a set of developmentally important genes (Surani, 1998). Because imprinted genes are regulated by these gametic epigenetic marks, and by further epigenetic modifications in the somatic cell, they are particularly vulnerable to environmentally induced mutation. One of the best studied epigenetic marks is DNA methylation. DNA methylation is established in either the maternal or paternal germline at discrete genomic loci. This methylation is preserved in the fertilized embryo to generate differentially methylated regions (DMRs) which then signal to nearby genes to establish domains of imprinted chromatin by mechanisms that are not fully understood (John and Lefebvre, 2011). These germline or gametic DMRs (gDMRs) can orchestrate the monoallelic expression of genes over megabases of DNA (Tomizawa *et al.*, 2011) and are reset with every reproductive cycle (Lucifero *et al.*, 2002; Obata and Kono, 2002).

The increased frequency of epimutation(s) at imprinted loci in ART infants has led to the suggestion that ART procedures may induce imprinting error(s). However, these studies are confounded because ART populations are, by their very nature, different from populations who were conceived without the use of ART, with a low fertility rate, an increased frequency of reproductive loss and usually of advanced age, all of which are associated with increased occurrence of fetal and neonatal abnormalities. Furthermore, it is difficult to determine the causality of imprinting errors in any specific abnormality reported after ART. Both IVF and ICSI appear to be associated with an increased relative risk of imprinting disorders (Savage *et al.*, 2011). These procedures are often undertaken for unexpected infertility and require ovarian stimulation, oocyte collection and *in vitro* culture before the embryos are implanted. It has been suggested that infertility and any resulting ovarian stimulation may predispose to epigenetic errors (Sato *et al.*, 2007). Animal studies suggest that *in vitro* embryo culture may be associated with epigenetic alterations. In particular, the large offspring syndrome in cattle undergoing ART is associated with the loss of maternal allele methylation at insulin-like growth factor 2 receptor (*IGF2R*) gDMR (Young *et al.*, 2001) and has phenotypic similarity to BWS. It is still unknown when these imprinting errors arise and what factors predispose to epigenetic changes. Previously, Chang *et al.* (2005) reported no phenotypic differences between BWS patients who were conceived after ART and naturally. However, Lim *et al.* (2009) reported that patients who were conceived after ART had a significantly lower frequency of exomphalos and higher risk of non-Wilms tumor neoplasia. Phenotypic differences between patients who were conceived after ART and naturally are largely unreported, while any changes to phenotype may be altered by the frequency and the degree of epimutations. Studies revealed that some patients with BWS born after ART presented with epimutations that were not restricted to the 11p15 region (Rossignol *et al.*, 2006; Bliek *et al.*, 2009; Lim *et al.*, 2009). Further analysis of abnormal methylation patterns in imprinting disorders may provide clues as to the cause of disease and identify the ART-related risk factor(s).

To address these questions in this study, we engaged in a nationwide epidemiological study of the Japanese population to determine the frequency of four imprinting disorders after natural conception and after ART. We then analyzed the DNA methylation status of 22 gDMRs in BWS and SRS patients conceived by the two routes. Finally, we compared the abnormal methylation patterns and the phenotypes reported for both sets of patients. As a result we found that both BWS and SRS were more frequent after ART and that ART patients exhibited a higher frequency of aberrant DNA methylation patterns at multiple loci with, in some cases, mosaic methylation errors.

Materials and Methods

Nationwide investigation of imprinting disorders

The protocol was established by the Research Committee on the Epidemiology of Intractable Diseases. The protocol consisted of a two-stage postal survey. The first-stage survey was used to estimate the number of individuals with any of the four imprinting diseases: BWS, SRS, PWS and AS. The second-stage survey was used to identify the clinico-epidemiological features of these syndromes.

In the first-stage survey, the pediatric departments of all hospitals were identified based on a listing of hospitals, as at 2008, supplied by the R&D Co. Ltd (Nagoya, Japan). Hospitals were classified into seven categories according to the type of institution and the number of hospital beds. The survey was mailed to a total of 3158 departments in October 2009 with letters of request for participation in recording these diseases. A simple questionnaire was used to ask about the number of patients with any of the four imprinting disorders. Diagnosis was determined by karyotype analyses, genetic analyses and clinical phenotypes by their clinical doctors. In December 2009, a second request was sent to departments that had not responded to the earlier deadline (at the end of November 2009). Following the first-stage survey, we sent acknowledgement letters to departments that had responded.

The second questionnaires were forwarded to the departments that had reported patients with the imprinting disorders on the first questionnaires. Detailed clinical information for the patients with these imprinting disorders was collected, including the age, gender, growth and development pattern, the methods of the diagnosis, the presence of infertility treatment and the methods of ART where applicable. Duplicate results were excluded using the information regarding the patient's age and gender where available. The study was approved by the Ethics Committee of Tohoku University School of Medicine.

Estimation of prevalence of imprinting disorders

The number of patients, who were diagnosed by genetic and cytogenetic testing and by clinical phenotypes, was obtained from data from the departments who responded to the first survey. The 95% confidence interval (CI) was calculated as previously described (Wakai *et al.*, 1997). The prevalence was determined, based on the population of Japan in 2009 (127 510 000) with data from the Statistics Bureau of the Ministry of Internal Affairs and Communications.

DNA preparation

Genomic DNA was obtained from blood or buccal mucosal cell samples from patients with one of the imprinting disorders using standard extraction methods (Kobayashi *et al.*, 2007). For control DNAs, DNA was prepared from the sperm and cord blood samples from unaffected individuals. The study was performed after obtaining patients or their parents' consent.

Bisulfite-treatment PCR including the SNPs

We first searched for single nucleotide polymorphisms (SNPs) within 22 previously reported human gDMRs (Kikyo *et al.*, 1997; Smith *et al.*, 2003; Kobayashi *et al.*, 2006, 2009; Wood *et al.*, 2007) using 20 control Japanese blood DNA samples. PCR primer sets were designed to span these SNPs (Supplementary data, Table SI) and human sperm DNA and blood DNA was used to confirm that these PCR assays detected the methylation status of the 22 DMRs. Paternal DMRs were shown to be fully methylated in sperm DNA, maternal DMRs were fully unmethylated and in blood DNA, both paternal and maternal DMRs showed ~50% methylation (Supplementary data, Fig. S1). The human gDMRs and the non-imprinted repetitive long interspersed nucleotide element (*LINE1*) and *Alu* repetitive sequences were examined by bisulfite sequencing using established protocols (Kobayashi *et al.*, 2007). Briefly, PCR products were purified and cloned into the pGEM-T vector (Promega, Madison, WI, USA). Individual clones were sequenced using M13 reverse primer and an automated ABI Prism 3130xl Genetic Analyzer (Applied Biosystems, Foster City, CA, USA). On average, 20 clones were sequenced for each sample.

Statistics

The frequency of the manifestation in patients who were conceived after ART was compared with that observed in patients conceived naturally using Fisher's exact test.

Results

Frequency of four imprinting disorders and their association with ART

We first investigated the nationwide frequency of four imprinting disorders (BWS, AS, PWS and SRS) in Japan in the year 2009. Of a total of 3158 departments contacted, 1602 responded to the first-stage survey questionnaire (50.7%). The total number of cases was calculated using a second-stage survey ensuring the exclusion of duplicates (Table I). Using this information, and taking into account the number of patients with suspect clinical signs but without a formal diagnosis, we identified 444 BWS patients (95% CI: 351–538), 949 AS patients (95% CI: 682–1217), 2070 PWS patients (95% CI: 1504–2636) and 326 SRS patients (95% CI: 235–416). From these figures (and using the 2009 population of Japan: 127 510 000) we estimated the prevalence of these syndromes to be 1 in 287 000, 1 in 134 000, 1 in 62 000 and 1 in 392 000, respectively, for BWS, AS, PWS and SRS. Further details are given in Supplementary data, Table SII and Supplementary data, Fig. S2.

Table I The 2009 frequency of four imprinting diseases in Japan in relation to use of assisted reproduction techniques (ART).

Imprinting disorders	Total estimated patient number (95% CI)	The total prevalence of the syndrome	The number of patients after ART/ total (%)
BWS	444 (351–538)	1 in 287 000	6/70 (8.6)
AS	949 (682–1217)	1 in 134 000	2/123 (1.6)
PWS	2070 (1504–2636)	1 in 62 000	4/261 (1.5)
SRS	326 (235–416)	1 in 392 000	4/42 (9.5)

Results of a nationwide epidemiological investigation of four imprinting disorders in Japan, under the governance of the Ministry of Health, Labor and Welfare of the Japanese government. Precise diagnosis was performed using fluorescence *in situ* hybridization and DNA methylation analyses. The type of ART, obtained from the questionnaires, was compared with the frequencies of these diseases and the epimutation rates. BWS, Beckwith-Wiedemann syndrome, AS, Angelman syndrome, PWS, Prader-Willi syndrome; SRS, Silver-Russell syndrome.

Between 1997 and 2008, the period during which the ART babies in this study were born, 0.64–0.98% of the total number of babies born in Japan were born as a result of IVF and ICSI. We ascertained the frequency of ART procedures in the cases of BWS, AS, PWS and SRS via the questionnaire sent to doctors (Table I, Supplementary data, Table SIII). The numbers of patients with PWS and AS we identified was low; however, the frequency of ART in these cases was not dissimilar to that expected, based on the population rate of ART use, with 2/123 (1.6%) cases of AS and 4/261 (1.5%) cases of PWS born after ART. In contrast, for BWS and SRS the frequency of ART was nearly 10-fold higher than anticipated with 6/70 (8.6%) BWS and 4/42 (9.5%) SRS patients born after ART.

After analyzing the second questionnaire, the blood or buccal mucosal cell samples were obtained from 15 individuals with BWS, 23 with SRS, 73 with AS and 29 with PWS. Using polymorphic bisulfite-PCR sequencing, we examined the methylation status of gDMRs within these samples at the imprinted regions implicated in these syndromes. For BWS we assayed *H19* and *KCNQ1OT1* (*LIT1*) gDMRs, for SRS we assayed the *H19* gDMR and for PWS and AS we assayed the *SNRPN* gDMR. For all patients (conceived naturally and with ART), the frequencies of DNA methylation errors (epimutations) corrected were 7/15 (46.7%) for BWS, 9/23 (39.1%) for SRS, 6/73 (8.2%) for AS and 2/29 (6.9%) for PWS. When looking at the ART cases exclusively, epimutation rates were 3/5 (BWS), 3/7 (SRS), 0/2 (AS) and 0/2 (PWS).

Abnormal methylation patterns in the ART and naturally conceived SRS patients with epimutations.

While hypomethylation of *H19* at chromosome 11 is known to be a frequent occurrence in SRS (Bliek *et al.*, 2006), various additional loci at chromosomes 7, 8, 15, 17 and 18 have been implicated as having a

role in this syndrome (OMIM 180860). We first identified SNPs in the previously reported 22 human DMRs using genomic DNA isolated from human sperm and blood from unaffected individuals, which could then be used in bisulfite-PCR methylation assays to assign methylation to the parental allele. We next collected a total of 15 SRS samples, including previously collected samples (ART: 2, naturally conceived: 4), which had DNA methylation errors at the paternal gDMR at *H19*. Five of these were born from ART and 10 were from natural conceptions. We analyzed and compared the DNA methylation status of the 3 other paternal gDMRs and the 19 maternal gDMRs (Supplementary data, Fig. S3, Table, Supplementary data, Table SIV). In four out of the five ART cases, DNA methylation errors were not restricted to the *H19* gDMR, and were present at both maternally and paternally methylated gDMRs. These four cases showed a mixture of hyper- and hypomethylation with mosaic (partial) patterns. In contrast, only 3 of the 10 naturally conceived patients showed DNA methylation errors at loci other than *H19* gDMR.

To determine whether DNA methylation errors occurred in patients at a broader level in the genomes, we assessed the methylation profiles of the non-imprinted *LINE1* and *Alu* elements. We examined a total of 28 CpG sites in a 413-bp fragment of *LINE1* and 12 CpG sites in a 152-bp fragment of *Alu* (Supplementary data, Table SIV), and no significant differences were found in the methylation ratios between patients conceived by ART and naturally.

The abnormal methylation pattern in BWS patients with epimutations

In BWS, hypermethylation of *H19* or hypomethylation of *KCNQ1OT1(LIT1)* at human chromosome 11 are both frequently reported (Choufani *et al.*, 2010). We collected seven BWS samples with DNA methylation errors of the *LIT1* gDMR, one of which was derived from ART patient and six from naturally conceived patients (Supplementary data, Fig. S3, Table II, Supplementary data, Table SIV). In the one ART (ICSI) case, we identified four additionally gDMR methylation errors, again present at both maternally and paternally methylated gDMRs and with mixed hyper- and hypomethylation patterns. Furthermore, the methylation error at the *NESPAS* DMR was mosaic in this patient. One of the six naturally BWS cases had similar changes. Although we had only one BWS case conceived by ART, widespread methylation errors were similar to those for the DNA methylation error pattern in SRS.

Phenotypic differences between ART patients and those conceived naturally

The increased frequency of DNA methylation errors at other loci in the ART cases suggested that the BWS and SRS cases born after ART might exhibit additional phenotypic characteristics. However, when we compared in detail the clinical features from both categories of conception (Supplementary data, Table SV), we found no major differences between ART and naturally conceived patients with BWS and SRS.

Discussion

Our key finding from this study was a possible association between ART and the imprinting disorders, BWS and SRS. We did not find a similar association with PWS and AS but our numbers were quite low in this study and a larger due to the questionnaire return rate and relative rarity of the diseases, international study will be required to reach definitive conclusions. Furthermore, factors such as PCR and/or cloning bias in the bisulfite method and correction for changing rate of ART over time must be considered when analyzing any results.

In addition to the possible association between ART and BWS/SRS, we observed a more widespread disruption of genomic imprints after ART. The increased frequency of imprinting disorders after ART shown by us and others is perhaps not surprising given the major epigenetic events that take place during early development at a time when the epigenome is most vulnerable. The process of ART exposes the developing epigenome to many external influences, which have been shown to influence the proper establishment and maintenance of genomic imprints, including hormone stimulation (Sato *et al.*, 2007), *in vitro* culturing (DeBaun *et al.*, 2003; Gicquel *et al.*, 2003; Maher *et al.*, 2003), cryopreservation (Emiliani *et al.*, 2000; Honda *et al.*, 2001) and the timing of embryo transfer (Shimizu *et al.*, 2004; Miura and Niikawa, 2005). Furthermore, we and others have also shown that some infertile males, particularly those with oligozoospermia, carry pre-existing imprinting errors in their sperm (Marques *et al.*, 2004; Kobayashi *et al.*, 2007; Marques *et al.*, 2008) which might account for the association between ART and imprinting disorders.

Imprinting syndromes and their association with ART

We report the first Japanese nationwide epidemiological study to examine four well-known imprinting diseases and their possible association with ART. We found that the frequency of ART use in both BWS and SRS was higher than anticipated based on the nationwide frequency of ART use at the time when these patients were born. Several other reports have raised concerns that children conceived by ART have an increased risk of disorders (Cox *et al.*, 2002; DeBaun *et al.*, 2003; Maher *et al.*, 2003; Orstavik *et al.*, 2003; Ludwig *et al.*, 2005; Lim and Maher, 2009). However, the association is not clear in every study (Lidegaard *et al.*, 2005; Doornbos *et al.*, 2007). The studies reporting an association were mainly from case reports or case series whereas the studies where no association was reported were cohort studies. Therefore, the differences in the epidemiological analytical methods might accounts for the disparity in findings.

Owing to the rare nature of the imprinting syndromes, statistical analysis is challenging. In addition, the diagnosis of imprinting diseases is not always clear cut. Many of the syndromes have a broad clinical spectrum, different molecular pathogenesis, and the infant has to have reached a certain age before these diseases become clinically detectable. It is therefore likely that some children with these diseases are not recorded with the specific diagnosis code for these syndromes. Nonetheless, in this study we were examining the relationship between ART and the imprinting syndromes and these confounding factors are likely to apply equally to both groups.

Both BWS and SRS occurred after ART but our numbers for PWS and AS were low, precluding any definitive conclusion for these two disorders. However, while most cases of BWS and SRS are caused by an epimutation, epimutations are very rare in PWS and AS (only 1–4%) and ART would not be expected to increase chromosome 15

Table II Abnormal methylation in patients with SRS and BWS.

Case	ART	Abnormal methylation			
SRS					
SRS-1	IVF-ET	H19 hypomethylated (mosaic)	PEG1 hypermethylated	PEG10 hypermethylated (mosaic)	GRB10 hypermethylated; ZNF597 hypomethylated
SRS-2	IVF-ET	H19 hypomethylated (mosaic)			
SRS-3	IVF-ET	H19 hypomethylated (mosaic)	PEG1 hypermethylated (mosaic)		
SRS-4	IVF-ET	H19 hypomethylated	GRB10 hypermethylated		
SRS-5	IVF-ET	H19 hypomethylated (mosaic)	INPP5F hypermethylated		
SRS-6		H19 hypomethylated			
SRS-7		H19 hypomethylated (mosaic)	ZNF597 hypermethylated (mosaic)	ZNF331 hypomethylated (mosaic)	
SRS-8		H19 hypomethylated			
SRS-9		H19 hypomethylated (mosaic)			
SRS-10		H19 hypomethylated			
SRS-11		H19 hypomethylated (mosaic)	PEG1 hypermethylated		
SRS-12		H19 hypomethylated			
SRS-13		H19 hypomethylated (mosaic)	FAM50B hypomethylated		
SRS-14		H19 hypomethylated			
SRS-15		H19 hypomethylated			
BWS					
BWS-1	ICSI	LIT1 hypomethylated	ZDBF2 hypermethylated	PEG1 hypermethylated	NESPAS hypomethylated (mosaic)
BWS-2		LIT1 hypomethylated			
BWS-3		LIT1 hypomethylated			
BWS-4		LIT1 hypomethylated			
BWS-5		LIT1 hypomethylated			
BWS-6		LIT1 hypomethylated	ZDBF2 hypomethylated	ZNF331 hypomethylated (mosaic)	
BWS-7		LIT1 hypomethylated			

ET, embryo transfer. Summary of the abnormal methylation patterns in the ART conceived and naturally conceived patients with Silver-Russell syndrome (SRS) and Beckwith-Wiedemann syndrome (BWS) with epimutations. Numbers in parentheses show the results of the methylation rates obtained using bisulfite-PCR sequencing. The % of DNA methylation of 22 gDMRs in all patients with SRS and BWS examined are presented in Supplementary data, Table SIV. Depictions in red represent DMRs normally exclusively methylated on the maternal allele, while blue represent paternally methylated sites.

deletions or uniparental disomy, consistent with our findings. Prior to this investigation, there was some evidence for an increased prevalence of BWS after ART but less evidence for an increased prevalence of SRS, with five SRS patients reported linked to ART (Svensson *et al.*, 2005; Bliek *et al.*, 2006; Kagami *et al.*, 2007; Galli-Tsinopoulou *et al.*, 2008). Our population-wide study provides evidence to suggest that both BWS and SRS occur more frequently after ART in the Japanese population.

Mechanisms of epimutation in the patients conceived by ART

By performing a comprehensive survey of all the known gDMRs in a number of patients with BWS and SRS, we found that multiple loci were more likely to be affected in ART cases than those conceived naturally. Lim *et al.* (2009) have reported a similarly increased frequency of multiple errors after ART, with 37.5% of patients conceived with ART and 6.4% of naturally conceived patients displaying abnormal methylation at additional imprinted loci. However, while Bliek *et al.* (2009) reported alterations in multiple imprinted loci in 17 patients out of 81 BWS cases with hypomethylation of *KCNQ1OT1*(*LIT1*) ICR, only 1 of the cases with multiple alterations was born after ART. Similarly, Rossignol *et al.* (2006) reported that 3 of 11 (27%) ART-conceived patients and 7 of 29 (24%) naturally conceived patients displayed abnormal methylation at additional loci. In these four earlier studies, not all gDMRs were assayed and it may be that by doing so, these incongruities will be resolved.

The pattern of cellular mosaicism we observed in some patients suggested that the imprinting defects occurred after fertilization rather than in the gamete as DNA methylation alterations arising in the gamete would be anticipated to be present in every somatic cell. This suggested the possibility that the DNA methylation errors occurred as a consequence of impaired maintenance of the germline imprints rather than a failure to establish these imprints in the germline or a loss of these imprints in the sperm or oocytes *in vitro*. Furthermore, some patients conceived by ART with SRS and BWS showed

alterations at both maternally and paternally methylated gDMRs suggesting that the defects were not limited to one parental germline. The mechanisms controlling the protection of imprinted loci against demethylation early in the development remain unclear. Our data suggested that this protection may fail in ART resulting in the tissue-specific loss of imprints, though it remains unclear if this ever occurs naturally. Potential factors involved could include the culture conditions for the newly fertilized oocyte and the length of exposure to specific media or growth factors, as part of the ART procedure. Some of the naturally conceived patients also had abnormal methylation at both maternally and paternally methylated gDMRs, which were in some cases mosaic. This could indicate that fertility issues arise as a consequence of pre-existing mutations in factors required to protect and maintain imprints early in life and it may therefore be possible to identify genetic mutations in these factors in this group of patients.

Clinical features

In our large-scale epidemiological study, we found differences in the frequency of some classic features of SRS and BWS between patients conceived by ART and those conceived naturally. We found that 7/7 (100%) ART conceived SRS patients showed body asymmetry, whereas only 30/54 (55.5%) who were conceived naturally possessed this feature. Similarly in BWS, earlobe creases were present in 4/7 (57.1%) ART conceived cases and 44/89 (49.4%) naturally conceived, bulging eyes in 3/7 (42.8%) versus 21/89 (23.6%), exomphalos in 6/7 (85.7%) versus 61/89 (68.5%) and nephromegaly in 2/7 (28.6%) versus 18/89 (20.2%), respectively. It is therefore possible that the dysregulation of the additional genes does modify the typical SRS and BWS phenotypes (Azzi *et al.*, 2010). BWS patients with multiple hypermethylation sites have been reported with complex clinical phenotypes (Bliek *et al.*, 2009) and a recently recognized BWS-like syndrome involving overgrowth with severe developmental delay was reported after IVF/ICSI (Shah *et al.*, 2006).

In our study patients with diagnosed imprinting disorders that presented with defects at additional loci (i.e. other than the domain responsible for that disorder) did not display additional phenotypes not normally reported in BWS or SRS. Since we were effectively selecting for classic cases of BWS and SRS in the first instance, it is possible that there are individuals born through ART showing entirely novel or confounding phenotypes that were not identified in our survey. Alternatively, as many of the alterations we observed showed a mosaic pattern, it is possible that mosaic individuals have more subtle phenotypes. In light of this new information on mosaicism, we may be able to use our knowledge of the individual's epigenotype to uncover these subtle changes.

This study, and the work of our colleagues, highlights the pressing need to conduct long-term international studies on ART treatment and the prevalence of imprinting disorders, particularly as the use of ART is increasing worldwide. It remains to be seen if other very rare epigenetic disorders will also have a possible association with the use of ART. Furthermore, it is not yet known what other pathologies might be influenced by ART. For example, in addition to general growth abnormalities, many imprint methylation errors also lead to the occurrence of various cancers (Okamoto *et al.*, 1997; Cui *et al.*, 1998). Further molecular studies will be required to understand the pathogenesis of these associations, and also to identify preventative methods to reduce the risk of occurrence of these syndromes following ART.

Supplementary data

Supplementary data are available at http://humrep.oxfordjournals.org/.

Acknowledgements

The authors thank the patients and their families who participated in this study. We are also grateful to the physicians who responded to the first and second surveys. We would like to thank Ms Chizuru Abe for technical assistance.

Authors' roles

H.H., H.O., N.M., F.S. and A.S. performed the DNA methylation analyses. M.K., K.N. and H.S. collected the samples of the patients. K.N. did the statistical analyses. H.H., M.V.D.P., R.M.J. and T.A. wrote this manuscript. All authors have read and approved the final manuscript.

Funding

This work was supported by Grants-in-Aid from the Ministry of Health, Labour and Welfare of the Japanese government (The Specified Disease Treatment Research Program; 162, 054) and Scientific Research (KAKENHI; 21028003, 23013003, 23390385), as well as the Uehara Memorial Foundation and Takeda Science Foundation (TA).

Conflict of interest

None declared.

References

Azzi S, Rossignol S, Le Bouc Y, Netchine I. Lessons from imprinted multilocus loss of methylation in human syndromes: A step toward understanding the mechanisms underlying these complex diseases. *Epigenetics* 2010;**5**:373–377.

Bliek J, Terhal P, van den Bogaard MJ, Maas S, Hamel B, Salieb-Beugelaar G, Simon M, Letteboer T, van der Smagt J, Kroes H *et al.* Hypomethylation of the H19 gene causes not only Silver-Russell syndrome (SRS) but also isolated asymmetry or an SRS-like phenotype. *Am J Hum Genet* 2006;**78**:604–614.

Bliek J, Verde G, Callaway J, Maas SM, De Crescenzo A, Sparago A, Cerrato F, Russo S, Ferraiuolo S, Rinaldi MM *et al.* Hypomethylation at multiple maternally methylated imprinted regions including PLAGL1 and GNAS loci in Beckwith-Wiedemann syndrome. *Eur J Hum Genet* 2009;**17**:611–619.

Bowdin S, Allen C, Kirby G, Brueton L, Afnan M, Barratt C, Kirkman-Brown J, Harrison R, Maher ER, Reardon W. A survey of assisted reproductive technology births and imprinting disorders. *Hum Reprod* 2007;**22**:3237–3240.

Chang AS, Moley KH, Wangler M, Feinberg AP, Debaun MR. Association between Beckwith-Wiedemann syndrome and assisted reproductive technology: a case series of 19 patients. *Fertil Steril* 2005;**83**:349–354.